

Single-Molecule Fullerenes: Current Stage and Perspective

Published as part of "Organic Functional Materials: Special Issue in Honor of Professor Daoben Zhu on His 80th Birthday".

Hanqiu Nie, Cong Zhao, Zujin Shi,* Chuancheng Jia,* and Xuefeng Guo*



Cite This: *ACS Materials Lett.* 2022, 4, 1037–1052



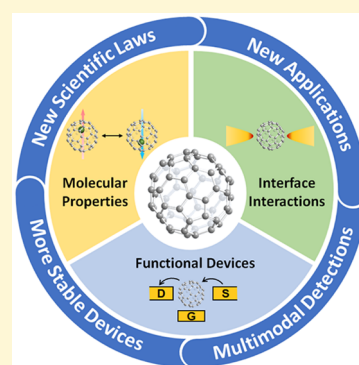
Read Online

ACCESS |

Metrics & More

Article Recommendations

ABSTRACT: Single-molecule techniques can reveal new fundamental physical and chemical effects of matters at the single-molecule scale, and build functional devices based on molecular properties to achieve specific optoelectronic functions. So far, various molecules have been introduced into single-molecule junctions to investigate their unique properties at the single-molecule scale. Among them, fullerene molecules, as a unique class of functional materials, provide infinite opportunities for fabricating various single-molecule devices. The combination of fullerenes and single-molecule electronic techniques not only realizes the discovery of new principles and new properties at the single-molecule scale, but also leads to the functionalization of single-molecule devices. This perspective discusses the properties of single fullerene molecules, such as charge transport, spin, nanomechanics, thermoelectricity, etc., introduces prototype functional devices based on the properties of single fullerene molecules, and provides directions for further research in this field.



1. INTRODUCTION

Single-molecule science, which focuses the study on the properties of individual molecules, has many important scientific significances.^{1–6} Specifically, single-molecule techniques can reveal new fundamental physical and chemical effects of materials at the single-molecule scale. For example, the quantum behavior determines the dominant properties of a system at the nanometer scale, which often leads to the properties that differ from the macroscopic system. Single-molecule measurements can rule out averaging effects, which originate from the observation of a large number of molecules at the same time, thus hiding detailed single-molecule signals. In addition, the physical and chemical processes over time can be monitored by single-molecule techniques, which can help reveal the dynamic processes at the single-molecule scale. Because of these advantages, single-molecule science provides a solid platform and a powerful tool for exploring fundamental physical and chemical principles from the bottom of space.

Several single-molecule techniques, including optical, mechanical, and electrical approaches, have been developed.^{7–11} In particular, single-molecule electrical techniques detect the physical and chemical process by measuring the current through the single-molecule junctions. For instance, single-molecule junctions can be used to measure the process of different novel physical effects, such as Coulomb blockade,¹²

Kondo effect,¹³ spin crossover effect,^{14,15} and stereoelectronic effect.^{16,17} One of the most attractive prospects of single-molecule electrical techniques is the construction of functional single-molecule devices.¹⁸ These single-molecule prototype devices can achieve functions beyond traditional electronic devices based on the properties of single molecules. To this end, single-molecule switches,^{19–21} rectifiers,^{22,23} and transistors^{24–26} have been fabricated and widely studied.²⁷ In this interdisciplinary field, one of the key factors is the selection of functional molecules. These smallest building blocks provide the versatility in structural design and material selection to achieve specific electronic properties and functions.²⁸ Therefore, the selection and synthesis of a series of functional molecules with controllable structures and rich properties is of great significance for the development of single-molecule optoelectronic devices.

Fullerenes with rich physical and chemical properties have received extensive research attention and applications since

Received: March 19, 2022

Accepted: April 18, 2022

their discovery in 1985.²⁹ The arc discharge method³⁰ makes it possible to prepare large amounts of fullerenes and endohedral fullerenes, and subsequently the chemical reactions of fullerenes have been extensively studied. Fullerenes represented by Buckminster fullerene C₆₀ and related structures, including endohedral fullerenes and fullerene derivatives, constitute a large family of fullerene materials. Fullerene science has become a new interdisciplinary subject involving chemistry, physics, and material science. Fullerene materials have a conjugated π -electron system. The intercalated atoms and external chemical modifications can tune the properties of energy levels and solubility, which make fullerene materials widely used in semiconductor devices, such as polymer solar cells,^{31–35} field-effect transistors,^{36–40} and various molecular electronic functional devices.^{41–45} Because of their structural stability and chemical modifiability, fullerenes have been introduced into various single-molecule systems to study their unique properties in the early development of single-molecule techniques.^{46–48} With the synthesis and characterization of a large number of fullerene materials,^{49,50} fullerenes and their derivatives have been not only introduced into single-molecule junctions as research objects to explore their physical and chemical properties, but also as functional centers to realize the functionalization of single-molecule devices.^{44,51–55}

Fullerene materials have a conjugated π -electron system. The intercalated atoms and external chemical modifications can tune the properties of energy levels and solubility, which make fullerene materials widely used in semiconductor devices, such as polymer solar cells, field-effect transistors, and various molecular electronic functional devices.

In this review article, we discuss the fabrication methods and properties of fullerene-based single-molecule junctions. Specifically, the fabrication techniques of single-molecule junctions are summarized, including the scanning tunneling microscopic break junction (STM-BJ), the mechanically controlled break junction (MCBJ), the electromigration junction (EMJ), and the carbon electrode-based junction. Based on these single-molecule techniques, the study of fullerene materials can be realized at the single-molecule scale. Properties of single fullerene molecules, such as charge transport, spin, and nanomechanics, are discussed in detail. In addition, functional devices based on the single-molecule properties of fullerenes are also introduced, including thermoelectric devices and single molecule switches. Finally, potential challenges in the development of fullerene single-molecule research are discussed, and solutions to overcome current obstacles and directions for further research are proposed.

2. ELECTRICAL SINGLE-MOLECULE TECHNIQUES

In the last two decades, a variety of techniques for measuring single-molecule electrical properties have been established, which provides a basis for detecting the properties of a single fullerene molecule and realizing functional applications based on a single fullerene molecule. The precise construction of

molecular-scale nanogaps is a key step in the fabrication of single-molecule devices. The break-junction technique is a powerful method to construct a molecular-scale gap. There are two main break-junction techniques: mechanical break junctions (Figure 1) and electrical break junctions (Figure 2). Using mechanical forces to construct molecular-scale gaps can enable the measurement of single molecules, especially the detection of charge transport through single molecules. This technique can be divided into two main types: scanning tunneling microscopic break junctions (STM-BJs; see Figures 1a and 1c) and mechanically controllable break junctions

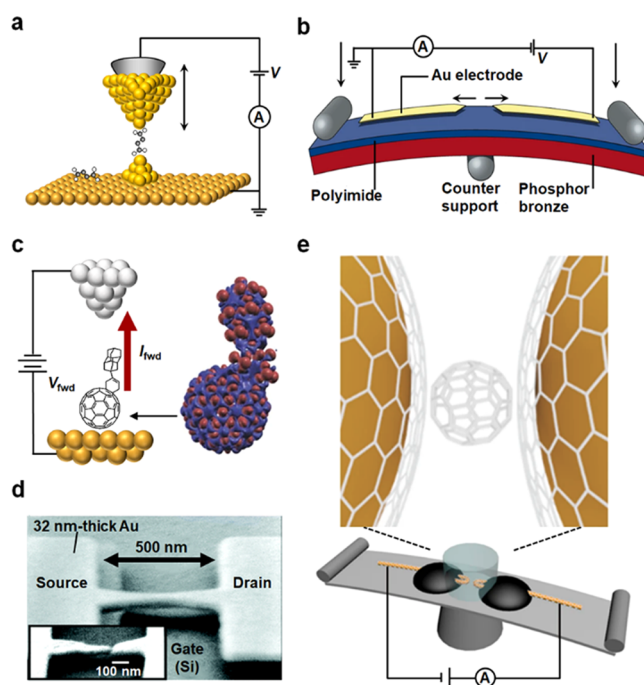


Figure 1. Single-molecule mechanical break junctions. (a) Schematic diagram of a scanning tunneling microscopic break junction (STM-BJ). (b) Schematic diagram of a mechanically controllable break junction (MCBJ). [Panels (a) and (b) have been reprinted with permission from ref 2. Copyright 2019, Springer Nature.] (c) Schematic illustration of a fullerene derivative in a STM-BJ. [Reprinted with permission from ref 56. Copyright 2014, Springer Nature.] (d) Scanning electron microscopic image of a MCBJ sample with a silicon substrate gate before and after the gold bridge fracture. [Reprinted with permission from ref 48. Copyright 2005, American Chemical Society, Washington, DC.] (e) Schematic illustration of a mechanically controllable break junction with graphene/single fullerene/graphene all-carbon components. [Reprinted with permission from ref 57. Copyright 2019, Springer Nature.]

(MCBJs; see Figures 1b, 1d, and 1e). In STM-BJ measurements, the metal tip and substrate first form metal-to-metal contact and then the tip is lifted slowly. During this process, the contact is broken and an atomic-scale tip is formed, which can pick up single molecules adsorbed on the substrate or dissolved in solution. The conductance of the single molecule in the junction between the substrate and tip is measured repeatedly, as a function of the distance; this is also called a breaking trace. Thousands of breaking traces statistically reveal the conductive characteristics of the molecule.

The principle of MCBJs is similar to that of STM-BJs. A MCBJ is based on the substrate bending caused by the

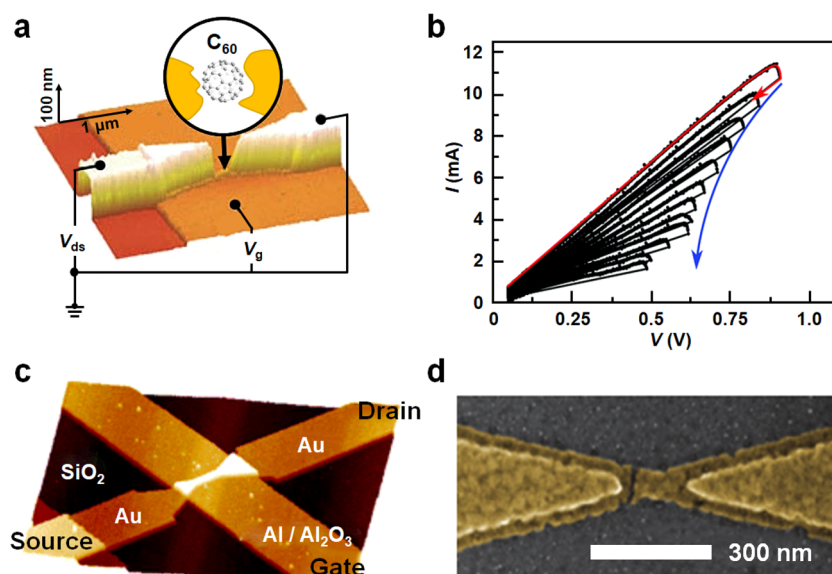


Figure 2. Single-molecule electromigration junctions. (a) Atomic force microscopy (AFM) image of the electromigration device with a C_{60} molecule trapped in the nanogap. [Reprinted with permission from ref 26. Copyright 2008, Springer Nature.] (b) Current–voltage (I – V) characteristics showing a typical active breaking scheme process. After that, few-atom-wide metal wire will break spontaneously to form a nano gap. [Reprinted with permission from ref 5. Copyright 2015, The Royal Society of Chemistry, London.] (c) AFM image of a continuous Au electrode, fabricated on top of an oxidized Al gate electrode before electromigration. [Reprinted with permission from ref 60. Copyright 2005, American Chemical Society, Washington, DC.] (d) Scanning electron microscopy (SEM) image of an aluminum nanogap obtained by electromigration of a constriction fabricated by angle evaporation. [Reprinted with permission from ref 61. Copyright 2009, Springer Nature.]

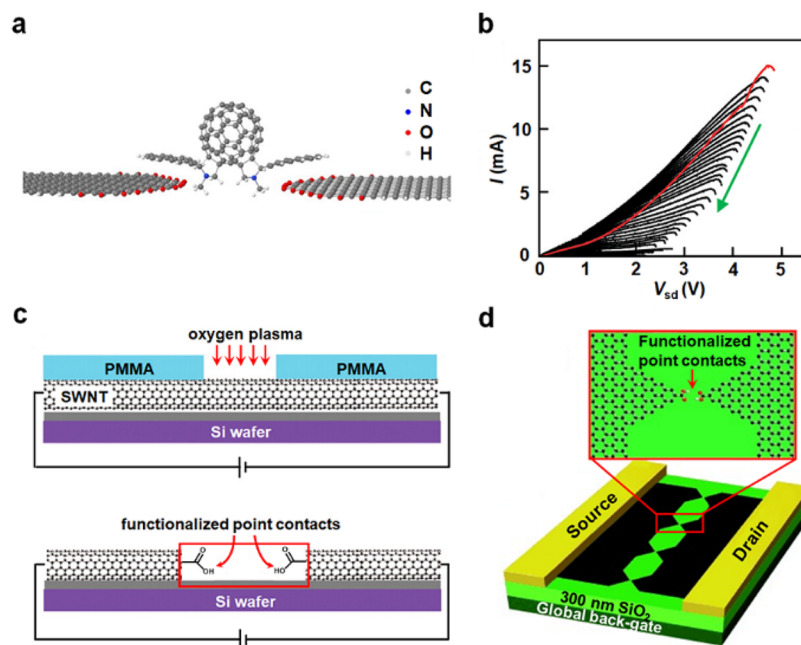


Figure 3. Carbon electrode-based single-molecule junctions. (a) Schematic diagram of π – π stacking interactions between the fullerene derivative and graphene electrodes fabricated using feedback-controlled electroburning of chemical vapor deposition grown graphene. [Reprinted with permission from ref 67. Copyright 2016, American Chemical Society, Washington, DC.] (b) Current–voltage (I – V) traces of the evolution (green arrow) of feedback-controlled electroburning in a graphene electrode. [Reprinted with permission from ref 68. Copyright 2011, American Chemical Society, Washington, DC.] (c) Precise fabrication of single-walled carbon nanotube nanoelectrodes with an oxygen plasma introduced through an opening in a window of PMMA defined with e-beam lithography. [Reprinted with permission from ref 69. Copyright 2006, AAAS.] (d) Indented graphene point contacts formed by oxidative cutting, which are functionalized by carboxylic acid end groups and separated by only a few nanometers. [Reprinted with permission from ref 70. Copyright 2012, Wiley–VCH Verlag GmbH & Co. KGaA, Weinheim, Germany.]

movement of an electrically driven pushing rod. The substrate bending indirectly displaces the positions of two free-standing

electrodes on the substrate, which fabricates a molecular-scale gap between sharp electrodes.^{58,59} The molecular-scale gap can

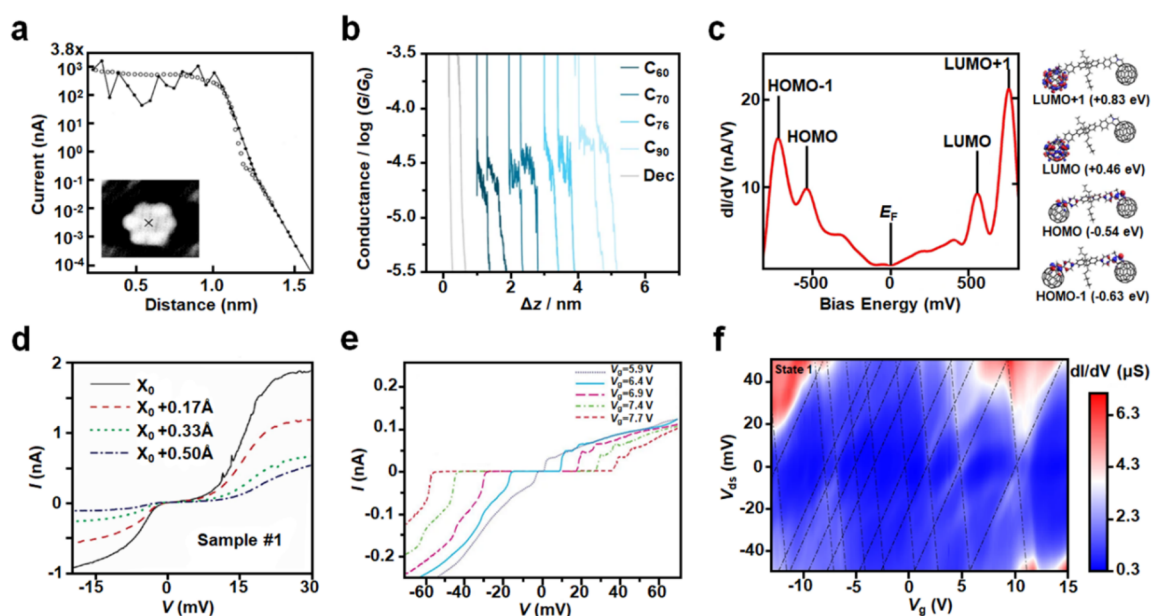


Figure 4. Charge transport of single fullerene molecules. (a) Tunneling current through a single C_{60} molecule, plotted as a function of the tip apex to the surface distance. Inset shows the measurement position, which is marked with a cross symbol (\times). [Reprinted with permission from ref 46. Copyright 1995, The American Physical Society.] (b) Typical single-molecule conductance–displacement curves for graphene/blank or single- C_{60} , C_{70} , C_{76} , and C_{90} /graphene junctions, which are measured by the MCBJ technique. [Reprinted by permission from ref 57. Copyright 2019, Springer Nature.] (c) dI/dV spectra and density functional theory (DFT)-calculated frontier molecular orbitals of a fullerene derivative. [Reprinted by permission from ref 81. Copyright 2016, Springer Nature.] (d) Current–voltage (I – V) curves at different source–drain displacements for a single C_{60} mechanically controllable break junction. [Reprinted with permission from ref 48. Copyright 2005, American Chemical Society, Washington, DC.] (e) I – V curves at different gate voltages in a single- C_{60} EMJ transistor. [Reprinted by permission from ref 47. Copyright 2000, Springer Nature.] (f) Conductance diagram plotted as a function of bias voltage and gate voltage in a $Gd@C_{82}$ single molecule EMJ transistor. [Reprinted with permission from ref 53. Copyright 2020, Springer Nature.]

be precisely controlled to achieve the mechanical stability by controlling the movement of the pushing rod indirectly. In addition, the breaking traces are also measured in the MCBJ approach. In comparison with the STM-BJ, the vertical movement of the pushing rod can be accurately controlled by a piezoelectric actuator or motor, which greatly improves the accuracy and stability of MCBJ devices. In combination with the gate fabrication process, the gate regulated three-terminal devices can be fabricated and tested with the MCBJ technique.⁴⁸

In the fabrication process of single-molecule junctions, the molecular-scale gap can be formed not only by the mechanical force, but also by the electric field force. Electrical break junctions are based on the electromigration process, so the technique is also called electromigration junctions (EMJs; see Figure 2a).^{47,62} This technique has two main issues that have attracted attention. One is the heating, and the other is the control of the gap size. Since Joule heating can activate the electromigration of contact atoms under a high current density, when a bias voltage increased in a ramp is applied to the thin metal wire, the wire breaks, forming two electrodes with a molecular-scale gap. The size of the gaps can be accurately controlled by the feedback control technique and a self-breaking technique (Figure 2b). The metal wire shrinks to a few atoms in size after electromigration, and then self-breaks at room temperature due to migration of surface atoms and the stress of materials, forming nanogapped electrode pairs.⁶³ Using this strategy, the formation of metal clusters caused by abrupt breakage can be avoided, improving the reliability of single-molecule junctions.⁶⁴ One of the advantages of EMJs is very compatible with the silicon technology, which provides an

opportunity to realize the integration of three-terminal devices with an electronic gate (Figure 2c). Since the electromigration process can occur in a variety of metal wires, it greatly expands the types of electromigration junctions and introduces electrode effects into single-molecule junctions. Different electrode materials have different coupling effects with molecules, which makes single-molecule devices exhibit the unique properties, such as proximity superconductivity (Figure 2d),^{61,65} magnetoresistance effect,⁶⁶ and so on.

Because of the migration of atoms along the surfaces at temperatures above ~ 200 K, Au EMJs become unstable at room temperature. Carbon materials are ideal alternative electrode materials that can avoid the instability problem at room temperature. The main fabrication methods of carbon electrodes mainly include electroburning and oxygen plasma etching, which remove excess carbon atoms by reaction with oxygen or sublimation under vacuum.^{68–73} The stable structure of the carbon framework and gaseous byproducts during the preparation also avoid the interference of cluster formation in metal electrode-based electromigration junctions. One of the connecting strategies between the single molecule and the electrodes involves the π – π stacking interaction (Figure 3a), which connects molecules by the interaction between graphene electrodes and the π -conjugated terminal group of molecules.^{55,67} Feedback control technique can control the size of the gaps accurately in this strategy (Figure 3b). Another connecting strategy is modifying the edge of graphene to form carboxyl groups. These carboxyl functional groups are formed by the oxidation of graphene under oxygen etching conditions (Figures 3c and 3d), which can form amide bonds with the target molecule to create a molecular junction

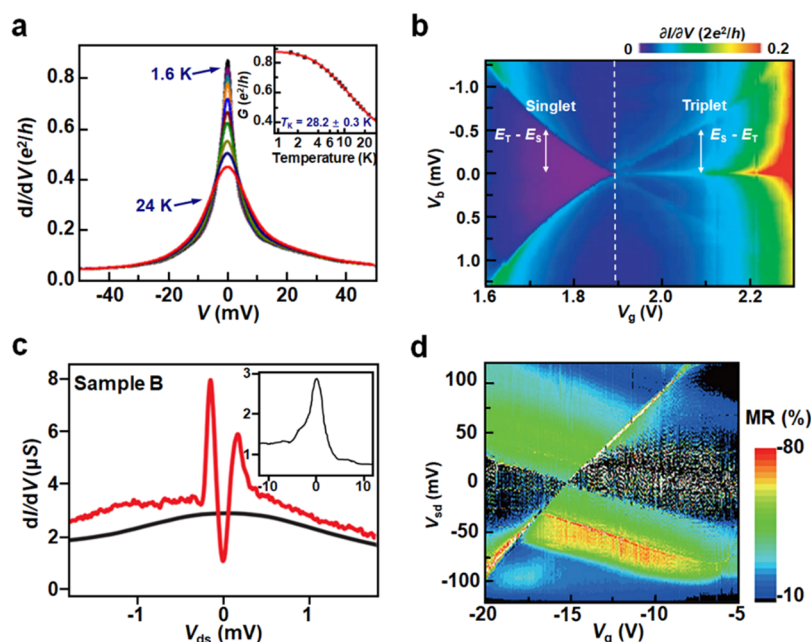


Figure 5. Spintronic characteristics of individual fullerene molecules. (a) Kondo effect in a C_{60} mechanically controllable break junction and the fit of the linear conductance with a Kondo temperature of 28.2 ± 0.3 K. [Reprinted with permission from ref 83. Copyright 2007, American Physical Society.] (b) Color map of the differential conductance (dI/dV), as a function of bias voltage and gate voltage in a single C_{60} transistor, showing the singlet to triplet spin transition. [Reprinted with permission from ref 26. Copyright 2008, Springer Nature.] (c) dI/dV , as a function of drain-source voltage at the normal (black line) and the superconducting state (red line) in a single C_{60} transistor. [Reprinted with permission from ref 61. Copyright 2009, Springer Nature.] (d) A color-coded spectrum of the tunnel magnetoresistance, as a function of bias voltage and gate voltage in a single C_{60} transistor with ferromagnetic electrodes. [Reprinted with permission from ref 66. Copyright 2013, American Chemical Society, Washington, DC.]

in chemical covalent binding. Based on the chemical bond connection, stable and reliable single-molecule functional devices could be achieved, such as molecular switch,^{21,74} single-molecule transistor,^{75,76} and chemical reaction detector.^{77–80}

3. CHARGE TRANSPORT OF SINGLE FULLERENE MOLECULES

The charge transport measurement of single fullerene molecules can be realized by the STM technology. The fullerene, C_{60} , is chosen as the research object, because of its relatively independent and stable molecular structure. For instance, the first study of the electrical contact between metal electrodes and an individual C_{60} molecule was performed by capturing a C_{60} molecule between a tungsten tip and the gold substrate in the STM.⁴⁶ The current as a function of tip displacements toward the molecule has been investigated to study the charge transport of single fullerene molecules (Figure 4a). The results show that the tunneling current increases approximately exponentially with the tip displacement in the tunneling regime, but this behavior changes significantly as the tip–molecule–substrate contact is established. Based on this change, the conductance of the molecule can be obtained. In addition, the conductivity of the single-molecule junction can be regulated by the size of the mechanically controlled gap in the MCBJ (Figure 4d), and the statistical measurement of fullerene conductance can also be realized by utilizing the MCBJ technique (Figure 4b).^{57,82,83}

By measuring the conductance properties of single fullerene molecules in different systems, the peaks in the differential conductance spectrum corresponding to molecular orbitals involved in the charge transfer process show the existence of a

Coulomb blockade effect.^{84–87} These charge transport properties are also observed in the junction based on fullerene derivatives (Figure 4c) and endohedral fullerenes. The external groups and encapsulated atoms/clusters can significantly affect the charge transport properties and mechanism. Electrodes also play an important role in the transport properties of single-molecule junctions. Replacing electrode materials can allow more research, such as molecular junctions with all carbon materials made of fullerenes and graphene electrodes.⁵⁷ The interaction between fullerene molecules and electrodes has developed a new molecular junction connection strategy, which utilizes fullerene terminals as anchoring groups. For example, a linear and rigid C_{60} capped molecule was designed for the connection of single-molecule junctions.⁸² The hybridization effect between fullerenes and metals makes fullerenes ideal materials as anchoring groups in single-molecule junctions. In comparison with the thiol anchoring group, the fullerene anchoring groups can significantly reduce the dispersion of low bias conductance. This connection strategy expands the potential application of fullerenes in the construction of single-molecule junctions.

Fullerenes are considered as a type of electron acceptors, because of their conjugated structures, which can accommodate multiple charges.^{88–91} This property makes it possible to fabricate single-molecule transistors by regulating the electron transport properties of fullerenes, especially through gate control. For instance, C_{60} -single-molecule transistors fabricated by the EMJ technique exhibit strongly suppressed conductance at near-zero bias voltages, followed by step-like current jumps at higher voltages, because of the Coulomb blockade effect.⁴⁷ The voltage range of the zero-conductance region can be regulated by the gate voltage (Figure 4e). Two-

dimensional conductance diagrams, plotted as a function of bias voltage and gate voltage in a Gd@C₈₂ single-molecule EMJ transistor, also showed the obvious Coulomb diamond (Figure 4f),⁵³ which proves that fullerene molecules can be effectively regulated by the gate electrode. Apart from using the EMJ technique, single-molecule transistors fabricated via the MCBJ technique can also realize the gate regulation of single molecules.⁴⁸ At the same time, the theoretical research provides a further understanding of fullerene molecules in single-molecule transistors. For example, a single-electron transistor based on C₆₀ molecules, which serve as quantum dots, exhibits a lower threshold voltage than that in the silicon-based transistor.⁹² Meanwhile, endohedral fullerenes with different inner atoms and clusters have different orbital energy levels, which can affect the gate regulation properties of the device.⁹³

In addition to the gate-regulated charge transport, the Coulomb blockade effect and electron transport properties are affected by the properties of fullerenes as well, such as the center of mass oscillation and inner atom vibration,^{47,60,94,95} and quantum phase transition.²⁶ The interaction between fullerenes and electrode materials, such as proximity superconductivity⁶¹ and magnetoresistance,^{66,96} will also couple or compete with Coulomb blockade effect, resulting in more novel phenomena.

4. SPINTRONIC CHARACTERISTICS OF SINGLE FULLERENE MOLECULES

Spintronics focuses on the spin properties of electrons, which may be applied to diverse fields, including information storage, quantum computing, molecular atomic clocks, and quantum metrology and sensing. In comparison with classical macroscopic spintronic devices based on traditional inorganic materials such as metals and semiconductors, single-molecule spintronic devices provide a new direction to develop the device miniaturization.⁹⁷

Furthermore, because of the weak spin orbit coupling of carbonaceous elements, fullerenes can keep the spin coherence state with a long relaxation time. Thus, fullerenes are considered as ideal materials for building spin quantum devices. At the molecular scale, many novel spin-related phenomena have been observed in single-molecule junctions, one of which is the Kondo effect. The Kondo effect refers to the interaction between spin electrons of molecules and electrons of electrodes, which can enhance the conductivity at near-zero bias voltages.⁹⁸ Therefore, the Kondo effect can be used to identify the presence of a net spin in the molecule. The spin of a molecule usually comes from the metal ion, but some nonmetal organic compounds are also magnetic molecules, because the partially filled orbital of the molecule offers a net spin.^{99,100} The Kondo effect of a single C₆₀ molecule (Figure 5a) has been observed in mechanically controllable break junctions.⁸³ This effect also promote the development of the research on many-body charge states, involving singlet–triplet quantum phase transitions (Figure 5b)²⁶ and interplay between superconductivity and molecular spins (Figure 5c).⁶¹ Among them, the interaction between spin electrons generated by magnetic electrodes and molecular spins produces interesting phenomena where the resistance of the molecule changes with the relative orientation reversal of the magnetization in the electrodes. According to this phenomenon, a single-molecule spin valve can be manufactured. For instance, ferromagnetic electrodes were introduced into the

C₆₀ electromigrated break junctions and split Kondo peaks were observed.⁹⁶ Single C₆₀ molecule transistors with ferromagnetic Ni electrodes were also fabricated to measure the gate-dependent magnetoresistance. The C₆₀ junctions exhibited a clear gate-dependent hysteretic tunnel magnetoresistance (TMR) and the TMR values reached as high as –80% (Figure 5d), which comes from an antiferromagnetic configuration generated by the hybridization between the states of the Ni substrate and the C₆₀ molecular orbitals. These advances demonstrate that the application of single fullerene molecules in spintronics is promising.

5. VIBRATIONAL CHARACTERISTICS OF SINGLE FULLERENE MOLECULES

When electrons pass through a single-molecule junction, vibrational modes of the molecules can influence the electron transport (Figure 6a). It is possible to observe the electron-

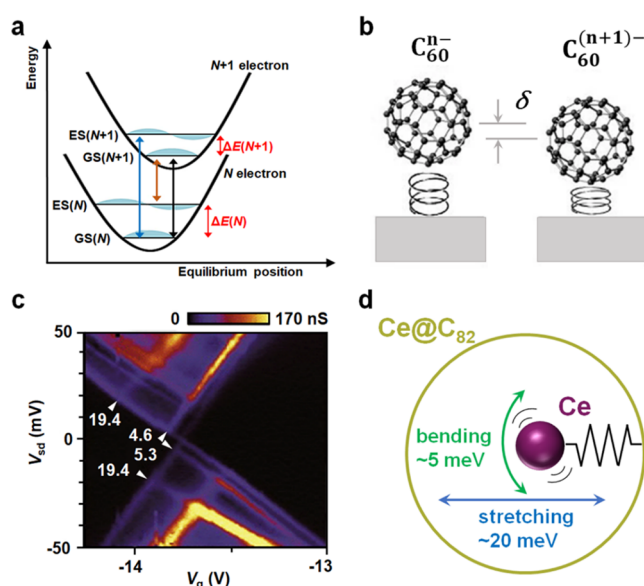


Figure 6. Vibrational characteristics in single molecule devices based on fullerene materials. (a) Schematic illustration of the vibronic energy diagram of the C₆₀ molecule in the nanogap. [Reprinted with permission from ref 95. Copyright 2018, Springer Nature.] (b) Schematic diagram of the center-of-mass oscillation of the electrostatic interaction between C₆₀ and electrodes. [Reprinted with permission from ref 47. Copyright 2000, Springer Nature.] (c) Coulomb stability diagram of a Ce@C₈₂ single-molecule transistor with excited-state lines marked by arrowheads and excited-state energies. (d) Schematic illustration of the vibrational modes of the Ce atom in Ce@C₈₂. [Panels (c) and (d) have been reprinted with permission from ref 94. Copyright 2015, AIP Publishing.]

vibration interactions in single-molecule devices. Through systematic studies, the electron transport mechanisms, molecular vibration modes, and nanomechanical oscillations of single fullerene junctions have been understood in detail. For instance, the charge transport measurements of a transistor based on the single C₆₀ molecule provide evidence for a coupling between the center-of-mass motion of the single C₆₀ molecule and single-electron hopping (Figure 6b).⁴⁷ According to the theory based on van der Waals and electrostatic interactions between the C₆₀ molecule and gold electrodes, the coupling is considered to be a quantized nanomechanical

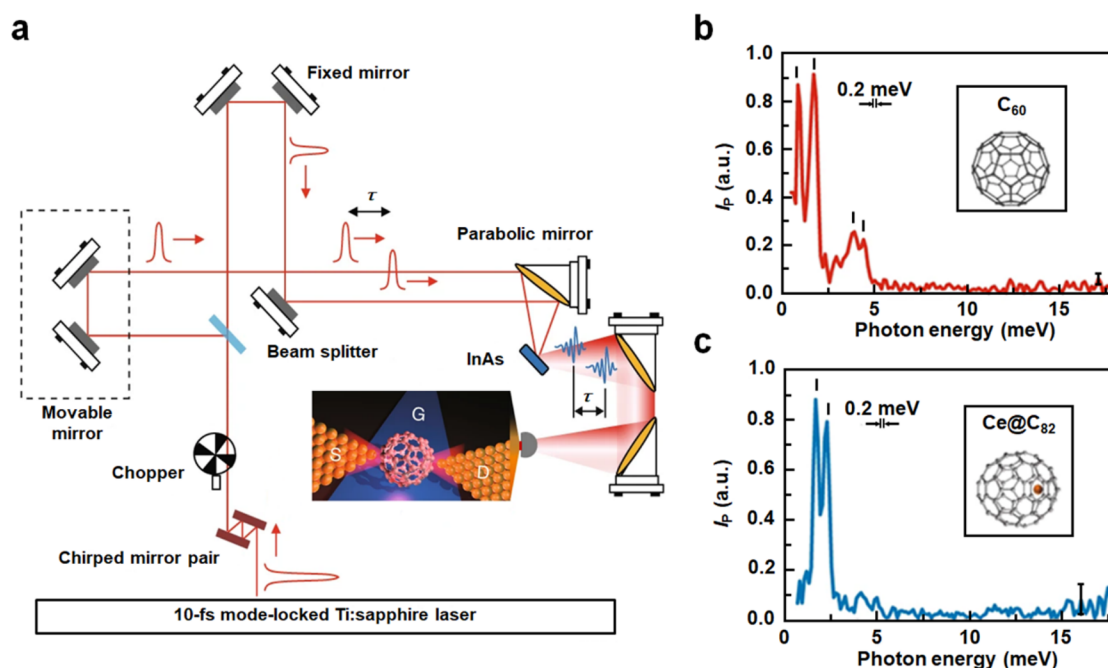


Figure 7. Terahertz spectra associated with the terahertz-induced center-of-mass oscillation of the fullerene molecules. (a) Schematic illustration of the single-molecule experimental setup of the terahertz spectroscopy composed of femtosecond laser pulses, the terahertz emitter, and the single-molecule transistor. (b, c) Fourier spectra of the interferogram for a C_{60} and $Ce@C_{82}$ single-molecule transistor, and terahertz spectra can be obtained by calculating the Fourier spectra of the interferogram. [Reprinted with permission from ref 95. Copyright 2018, Springer Nature.]

oscillation of the C_{60} molecule on the gold surface. Furthermore, the C_{60} internal deformation vibrational mode from a sphere to a prolate ellipsoid can be also observed. In a single-molecule transistor based on the C_{140} molecule with a mass-spring-mass geometry, the vibration-assisted tunneling at certain energy decided by the stretching mode is also observed.⁶⁰ The molecular electron-vibration coupling model explains that the interstage stretching mode is more strongly coupled to electron tunneling than that coupled to other internal modes of the molecule. For endohedral fullerenes, vibrations of internal atoms and clusters can also be monitored through the single-molecule electrical platform. For instance, the electron transport in single-molecule transistors based on endohedral metallofullerene $Ce@C_{82}$ and hollow fullerene C_{84} provide evidence for different types of vibrations (Figures 6c and 6d). The bending and stretching vibrational modes of a single Ce atom encapsulated in a C_{82} cage appear in the Coulomb stability diagram of single-electron tunneling through a single $Ce@C_{82}$ molecule. This result shows the great single-atom sensitivity of the transport measurement.

Experiments and theories have shown that some vibrational modes of fullerenes are in the terahertz band. The development of the terahertz spectroscopy, in combination with single-molecule devices, has made it possible to achieve a high temporal resolution detection of the electronic and vibrational properties of single molecules (Figure 7a). Terahertz-induced photocurrent associated with the terahertz-induced center-of-mass oscillation of the fullerene molecules has been obtained from the time-domain terahertz autocorrelation measurements.⁹⁵ The peaks were observed in the Fourier spectra of the interferogram for C_{60} junctions (Figure 7b) and similar sharp peaks were also observed in an endohedral metallofullerene $Ce@C_{82}$ molecule (Figure 7c). The observed low-energy excitations reflect the vibron-assisted tunneling process

promoted by the terahertz-induced center-of-mass oscillation of the C_{60} molecule. Therefore, the terahertz-induced single-molecule photocurrent detection system can achieve ultrahigh sensitivity detection of the electronic/vibrational structure in the process of adding or removing one electron in single fullerene molecules.

6. THERMOELECTRIC EFFECTS OF SINGLE FULLERENE MOLECULES

The thermoelectric effect describes the direct conversion of the temperature difference to the electric voltage. When there is a temperature difference between two points of a conductive material, the phenomenon of generating an electric potential between them is called the Seebeck effect, and the reverse conversion is called the Peltier effect. Specifically, the thermoelectric efficiency is expressed by the dimensionless factor $ZT = GS^2T/\kappa$, where S represents the Seebeck coefficient, T represents the average temperature, G represents the conductance and κ represents the sum of the contributions of electrons and phonons to the thermal conductance. Different from the mutual restriction between S , G , and κ in bulk materials, they can be improved at the same time in single-molecule devices. The theoretical derivation shows that the system with a discrete electron density of states may have the highest ZT value.¹⁰¹ Thus, the single-molecule junction, in which the energy levels of single molecules are discrete and quantized, is an ideal platform to study the thermoelectric effects at the single-molecule scale.^{102–104}

Fullerene molecules are highly conjugated and possess unique properties that are critical for achieving high thermoelectric conversion, including small HOMO–LUMO gaps and degenerated orbitals attributed to the high symmetry.^{105,106} These characteristics make fullerenes the material of choice in much single-molecule thermoelectric research. For instance,

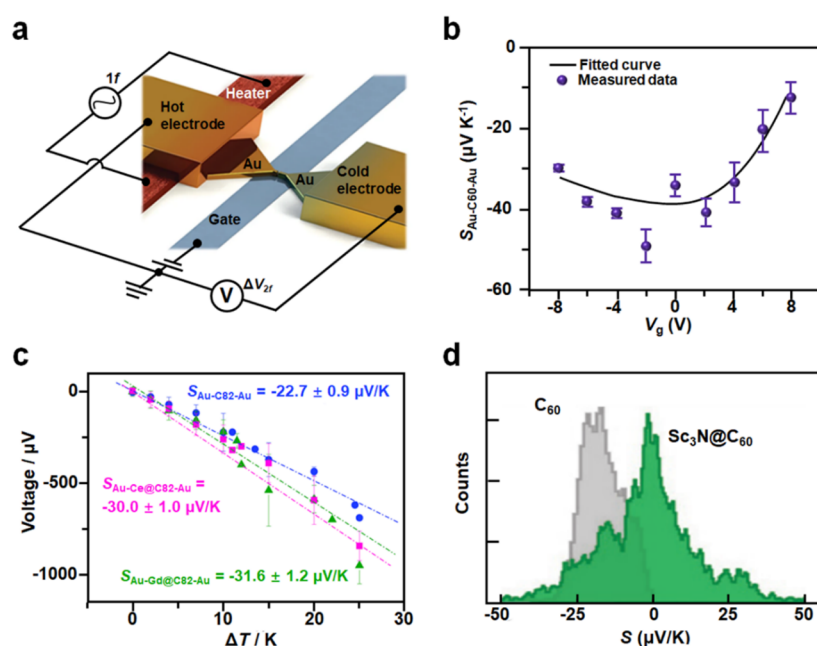


Figure 8. Thermoelectric effect in single-molecule devices based on fullerene materials. (a) Schematic diagram of the electromigrated break junction with integrated heater. (b) Seebeck coefficient of the Au–C₆₀–Au junction, as a function of V_g . [Panels (a) and (b) have been reprinted with permission from ref 54. Copyright 2014, Springer Nature.] (c) Thermoelectric voltage as a function of ΔT for C₈₂, Gd@C₈₂, and Ce@C₈₂ single-molecule junctions. [Reprinted with permission from ref 43. Copyright 2015, The Royal Society of Chemistry, London.] (d) Histograms of thermopower S for C₆₀ and Sc₃N@C₈₀. [Reprinted with permission from ref 44. Copyright 2015, Springer Nature.]

the electrostatic control of thermoelectric properties was realized in a single-molecule Au–fullerene–Au junction with a gate electrode (see Figures 8a and 8b).⁵⁴ The Seebeck coefficient and the electrical conductance of single-molecule junctions can be simultaneously increased by electrostatic control. From the study of single fullerene junctions, the enhanced thermoelectric performance can be attributed to the fact that the dominant transport orbital is located close to the Fermi level of the electrodes. In addition, electrostatically controlled thermoelectric properties are also observed in a single-molecule transistor composed of graphene electrodes.⁵⁵ Since the graphene electrodes reduce the shielding effect on the gate in comparison with the metal electrodes, the power factor of the graphene–fullerene junction can be tuned to a value close to the theoretical limit of the isolated Breit–Wigner resonance.

For endohedral fullerenes, the encapsulated atom can shift the energy level of the molecular orbitals, resulting in a thermoelectric effect different from that of hollow fullerenes. For instance, the different thermoelectric transport properties between endohedral fullerenes and hollow fullerenes have been studied in single-molecule junctions based on C₈₂, Gd@C₈₂, and Ce@C₈₂ molecules, respectively (Figure 8c).⁴³ The measurements of three STM-BJ devices and theoretical calculation results show n -conducting properties and a negative thermopower, which has a much larger absolute value for the Gd@C₈₂ and Ce@C₈₂ junctions. The enhancement of the thermopower for the endohedral fullerenes can be elucidated by the changes in the electronic and geometrical structure of the fullerene cages induced by the encapsulated metal atoms. The thermoelectric transport properties of the endohedral fullerene Sc₃N@C₈₀ have also been explored.⁴⁴ Different from Gd@C₈₂ and Ce@C₈₂ molecules, the magnitude and sign of the thermopower are strongly dependent on the orientation of the Sc₃N@C₈₀ molecule. The calculated results show that the

inner cluster Sc₃N has a sharp resonance near the Fermi level. These results indicate that Sc₃N@C₈₀ is a bithermoelectric material (Figure 8d), exhibiting both positive and negative Seebeck coefficients.

7. NANOMECHANICAL MOTION-INDUCED SINGLE-MOLECULE SWITCHING

Some evidence supports the fact that the metal atoms inside the cage of some endohedral fullerenes keep moving in the limited cage space at room temperature.^{107–109} Switching between bistate or multistate of molecules by controlling the nanomechanical motion of encapsulated atoms or cluster shows the potential of incorporating endohedral fullerenes into single-molecule switches and multistates memory. Many external factors can affect nanomechanical motion, and furthermore affect the state of molecules. For example, the chemical modification with an electron-donating group significantly changes the charge states of the cage, and the motion of inner atoms can also change the fullerenes without chemical modification.^{110,111} Moreover, when the metal electrode is in contact with a fullerene, the metal electrodes act both as a transport path of the conductive path and as a type of chemical modification for the fullerenes. Ab initio calculation results show that both the positions of the La atoms and the electronic transport through La₂@C₈₀–metal single-molecule junctions are largely influenced by the metallic electrodes.¹¹² Meanwhile, the internal motion of La atoms in La₂@C₈₀ is restricted in a charge-transfer process, which is highly influenced by the total charge and the tip–molecule–surface geometries of the nanobridge. By combining electronic structure calculations with dynamical simulations, the current-triggered dynamics in endohedral fullerene molecular junctions is studied.¹¹³ In the Au–Li@C₆₀–Au single-molecule junction, inelastic electron tunneling through a Li atom localized resonance shows that the Li atom exhibits a large amplitude

oscillation, with respect to the fullerene wall. In addition, the bounce motion of the fullerene cage between the Au electrodes is slightly influenced by the inner atom motion, based on the electronic actuation of the internal atom/cluster motion within a fullerene cage. These theoretical works confirm the potential application of fullerene materials in single-molecule switches based on inner atoms and clusters orientational configurations.

Using a low-temperature ultrahigh-vacuum scanning tunneling microscopic technique, switching configurations of molecular orientations have been observed in endohedral metallofullerene single-molecule junctions. For instance, the hysteresis including the negative differential conductance in the Tb@C₈₂ endohedral metallofullerene has been observed (Figures 9a and 9b).¹¹⁴ An octanethiol self-assembled

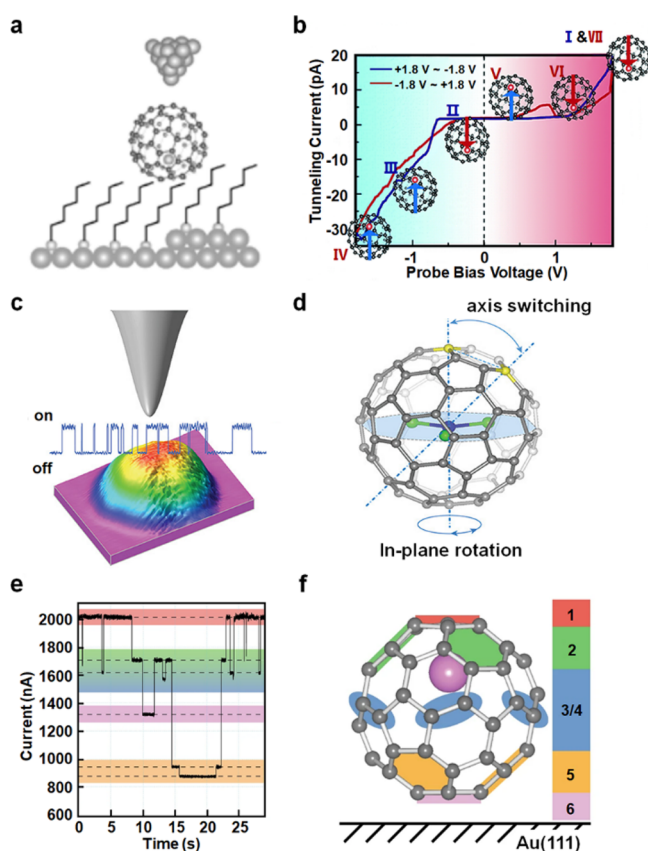


Figure 9. Nanomechanical motions of fullerene materials on single-molecule devices. (a) Schematic diagram of a double-barrier tunnel junction that consists of the PtIr/vacuum/Tb@C₈₂/hexanethiol SAM/Au. (b) Current–voltage (*I*–*V*) curves in different scanning directions and schematic diagram of single molecular orientation switching of Tb@C₈₂. [Panels (a) and (b) have been reprinted with permission from ref 114. Copyright 2005, American Chemical Society, Washington, DC.] (c) Three-dimensional pseudo color plot of Sc₃N@C₈₀ and the current switching behavior between two stationary states. (d) Determination of the Sc₃N motions associated with the switching events. [Panels (c) and (d) have been reprinted with permission from ref 115. Copyright 2011, American Chemical Society, Washington, DC.] (e) Current–time spectrum illustrating conductance changes of the Li@C₆₀ junction. The reversible alterations in conductance are confined to several distinct levels. (f) Schematic diagram of corresponding positions of Li atoms in the cage. [Panels (e) and (f) have been reprinted with permission from ref 51. Copyright 2019, Springer Nature.]

monolayer (SAM) is introduced between Tb@C₈₂ and the Au(111) substrate to control the thermal rotational states. The tunneling current shows different paths in the positive and negative scanning directions, in which there are peaks of the negative differential conductance. The observed hysteresis is interpreted by the switching of the Tb@C₈₂ molecular orientation caused by the interaction between its electric dipole moment and an external electric field. In addition, the rotational motion of the clusters in the cage can also be used as a single-molecule switch, such as a single-molecule switch based on the tunneling electron-driven rotation of a triangular Sc₃N cluster within a C₈₀ fullerene cage (Figure 9c).¹¹⁵ The antisymmetric stretching vibration of the Sc₃N cluster plays the role of the gateway to transfer energy from tunneling electrons to cluster rotation, as verified by the bias-dependent action spectra and modeling (Figure 9d). In addition to the bistate switching, fullerenes can also be applied to multistate switching. Based on low-temperature scanning tunneling microscopy and spectroscopy, up to 14 molecular states can be statistically observed in a multistate single-molecule switch using the endohedral fullerene Li@C₆₀ (Figure 9e).⁵¹ The switching mechanism is that the resonant tunneling via the superatom molecular orbitals of the fullerene cage activates the different site orientations of Li atoms (Figure 9f). These studies based on the STM technology demonstrate that endohedral fullerene single-molecule switches offer an opportunity to switch conductivity between multiple stationary states while remaining intact.

In addition to switching between polymorphisms, maintaining the stability in a specific state is also an important factor for single-molecule switching. The interaction between the gate electric field and the molecular dipole provides an idea for this regulation. In the electromigration single-molecule junction based on a single endohedral fullerene, the switching between two electric dipole states controlled by gate voltages can be realized (Figure 10a).⁵³ For instance, a gate-controlled switching between two electronic states has been observed in a single Gd@C₈₂ molecule. Gate voltages of ±11 V can switch the system between the two transport channels, resulting in a ferroelectricity-like hysteresis loop (Figure 10b). The two states are assigned to two different permanent electrical dipole orientations generated from the trapping of the Gd atom at two different sites inside the C₈₂ cage, and the two dipole states are separated by a transition energy barrier of 11 meV. The electric field-driven reorientation of the individual dipole results in conductance switching, as the coercive field provides the energy needed to overcome the transition barrier (Figure 10c). These studies demonstrate that endohedral fullerenes have the potential to be used to fabricate single-molecule functional devices in integrated electronics.

8. CONCLUSION AND OUTLOOK

Fullerene molecules provide a large class of alternative molecules for single-molecule devices, because of their unique properties. This paper reviews the representative work in the field of fullerene single molecules in recent years. First, different types of single-molecule electrical techniques are introduced, including mechanical break junctions, electromigration junctions, and carbon electrode single-molecule junctions. Specifically, the preparation principle and process of different single-molecule devices, as well as various components and characteristics in single-molecule detection are discussed in detail, which provides test platforms and detection

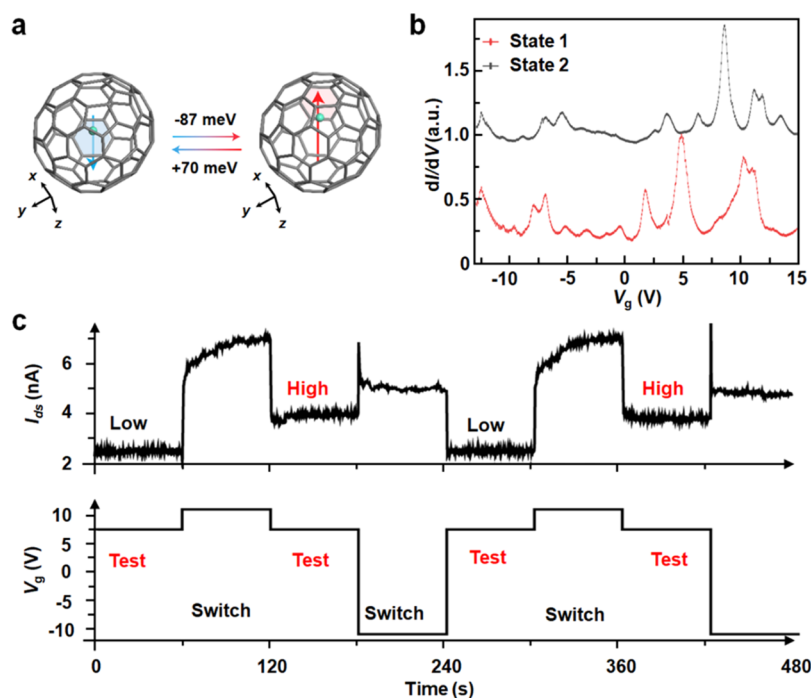


Figure 10. Gate-controlled switching in a Gd@C₈₂ single molecule device. (a) Schematic diagram of the switching interpreted as a transition between two configurations. (b) The source–drain current curve plotted as a function of the gate voltage, which was swept backward and forward. (c) Simulating a two-resistance-state operation based on the single-molecule switching at switching gate voltages of ± 11 V and a test gate voltage of 7.472 V. [Reprinted by permission from ref 53. Copyright 2020, Springer Nature.]

methods for the study of single fullerene molecules. Then, the properties of single fullerene molecules are introduced, such as Coulomb blockade effect, vibrational property, thermoelectric effect, orientation switching, and so on. The exploration of interactions between fullerenes and electrodes is also discussed, including the Kondo effect, quantum phase transition, proximity superconductivity, and magnetoresistance. Finally, on the basis of these properties, some single-molecule prototype functional devices are proposed. With the intersection of fullerenes and single-molecule techniques, many inherent, novel, and meaningful principles can be discovered by studying the fundamental mechanisms of single-molecule physics and chemistry. On the other hand, the rich properties and huge family of fullerenes provide a large number of alternative functional molecules for devices, which can realize more sensitive and efficient single-molecule functional devices.

With the synthesis and characterization of a large number of fullerene materials, fullerene science is changing from basic research focusing on the synthesis and structural characterization of new systems to the application of fullerenes and their derivatives. However, the application of single fullerene molecules, especially the application of single-molecule functional devices based on single molecular properties, is still insufficient. The field of fullerene single-molecule research still

The field of fullerene single-molecule research still faces many challenges in the improvement of the preparation technique, the expansion of the detection system and the wide application of the research results.

faces many challenges in the improvement of the preparation technique, the expansion of the detection system and the wide application of the research results.

First, fabricating stable and reliable single-molecule devices is one of the main challenges. Fullerene materials have been widely used in semiconductor devices. Based on SAM devices,^{116–118} many studies have also explored the properties and applications of fullerene materials at the molecular scale.^{42,119–127} In contrast, the fabrication of single-molecule devices with a single fullerene molecule as the functional center is more challenging. Although there are many techniques for fabricating single-molecule devices, it is difficult for these devices to be stable, reliable, and reproducible. By improving single-molecule device fabrication techniques, such as the use of new electromigration or etching techniques, it is expected to improve the yield of single-molecule junctions and enable device array fabrication. The single-molecule devices based on metal electrodes are not stable enough and may be damaged by the atomic migration of the electrodes. Because of the stability of carbon materials such as carbon nanotube and graphene, carbon materials are alternative electrode materials. In addition, improving the connection form of single molecules, introducing reliable anchor groups through molecular design, or connecting with strong chemical bonds can improve the stability of single-molecule devices.

Second, the regulation and detection methods of single fullerene molecules should be expanded. Single-molecule electrical characterization techniques can not only measure the charge transport and gate regulation of molecules under electric fields, but also enable the study of spintronics. However, fullerenes still have many important properties that cannot be studied by electrical modulation and detection methods. Therefore, it is necessary to develop single-molecule monitoring platforms with multiple regulation and detection

methods. Through a variety of regulation and multimodal detection methods, multilevel molecular information can be obtained. For example, new stimulation methods can be introduced, including polarized light, terahertz, femtosecond lasers, etc. Detection capabilities can be expanded by combining other single-molecule detection techniques, such as optical and mechanical single-molecule detection methods. In addition, for single-molecule junctions of electrical monitoring, improving the temporal resolution and signal-to-noise ratio is also one of the important development directions. It is expected to achieve this goal in combination with ultrafast electrical and ultrafast optical detection methods. Combining ultrafast electrical and ultrafast optical detection methods holds promise for monitoring ultrafast dynamics of single fullerene molecules.

Third, new principles and applications based on the properties of fullerenes should be explored. In recent years, a large number of endohedral fullerenes encapsulating magnetic atoms have been studied as single-molecule magnets.^{128–132} The fullerene cage can significantly reduce the relaxation processes associated with environmental fluctuations, and the carbonaceous elemental composition can effectively preserve spin coherence due to the zero nuclear spin of ¹²C, leading to the emergence of quantum states with long spin coherence.^{133–139} In combination with single-molecule devices, these fullerenes hold promise for a variety of quantum spin applications, including quantum computing,^{140,141} atomic clock,¹⁴² and quantum metrology and sensing.^{33,143} The atoms/clusters encapsulated in the carbon cages are good samples to study the unusual valence states,¹⁴⁴ confined interactions and motions.^{145–149} The atoms/clusters encapsulated in the carbon cages are good samples to study the unusual valence states,¹⁴⁴ as well as confined interactions and motions.^{145–149} These will greatly expand the application prospects of fullerenes and single-molecule devices.

AUTHOR INFORMATION

Corresponding Authors

Xuefeng Guo – Beijing National Laboratory for Molecular Sciences, National Biomedical Imaging Center, College of Chemistry and Molecular Engineering, Peking University, Haidian District, Beijing 100871, People's Republic of China; Center of Single-Molecule Sciences, Institute of Modern Optics, Frontiers Science Center for New Organic Matter, College of Electronic Information and Optical Engineering, Nankai University, Jinnan District, Tianjin 300350, People's Republic of China; orcid.org/0000-0001-5723-8528; Email: guoxf@pku.edu.cn

Chuancheng Jia – Beijing National Laboratory for Molecular Sciences, National Biomedical Imaging Center, College of Chemistry and Molecular Engineering, Peking University, Haidian District, Beijing 100871, People's Republic of China; Center of Single-Molecule Sciences, Institute of Modern Optics, Frontiers Science Center for New Organic Matter, College of Electronic Information and Optical Engineering, Nankai University, Jinnan District, Tianjin 300350, People's Republic of China; Email: jiacc@nankai.edu.cn

Zujin Shi – Beijing National Laboratory for Molecular Sciences, National Biomedical Imaging Center, College of Chemistry and Molecular Engineering, Peking University, Haidian District, Beijing 100871, People's Republic of China; orcid.org/0000-0003-0268-4584; Email: zjshi@pku.edu.cn

Authors

Hanqiu Nie – Beijing National Laboratory for Molecular Sciences, National Biomedical Imaging Center, College of Chemistry and Molecular Engineering, Peking University, Haidian District, Beijing 100871, People's Republic of China
Cong Zhao – Center of Single-Molecule Sciences, Institute of Modern Optics, Frontiers Science Center for New Organic Matter, College of Electronic Information and Optical Engineering, Nankai University, Jinnan District, Tianjin 300350, People's Republic of China

Complete contact information is available at:
<https://pubs.acs.org/10.1021/acsmaterialslett.2c00247>

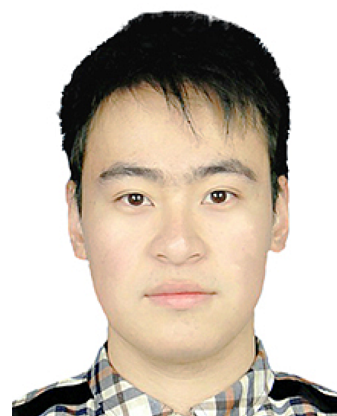
Author Contributions

All authors wrote the manuscript and approved the final version of the manuscript together.

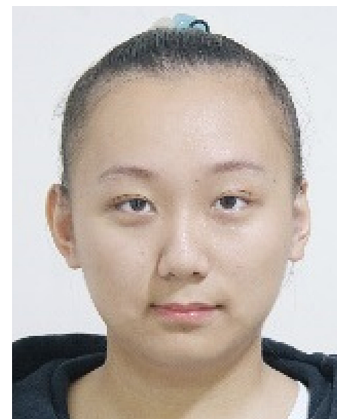
Notes

The authors declare no competing financial interest.

Biographies



Hanqiu Nie received his B.S. degree in 2019 from the College of Chemistry and Molecular Sciences, Wuhan University. He is currently a Ph.D. candidate at the College of Chemistry and Molecular Engineering, Peking University, under the guidance of Prof. Xuefeng Guo and Prof. Zujin Shi. His current research is focused on single-molecule dynamics.



Cong Zhao is currently a Ph.D. candidate in the Center of Single-Molecule Sciences, Institute of Modern Optics, College of Electronic Information and Optical Engineering, Nankai University, under the guidance of Prof. Xuefeng Guo. Her research is focused on single-molecule device physics and dynamics.



Zujin Shi graduated on Chemistry from Lishui Teacher's College in 1983; he received his M.Sc. degree in 1991 from Beijing Normal University and his Ph.D. degree in 1996 from Peking University. He was a postdoc at Peking University from 1996 to 1998 and a JSPS fellow at Nagoya University, Japan, from 2001 to 2002, respectively. He joined the faculty in 1998 and became a full professor in 2007 at Peking University. His current research is focused on nanocarbon materials and chemistry.



Chuancheng Jia received his Ph.D. degree in 2014 from the College of Chemistry and Molecular Engineering, Peking University, under the guidance of Prof. Xuefeng Guo. From 2014 to 2020, he was a postdoc at Institute of Chemistry, Chinese Academy of Sciences and University of California, Los Angeles. He joined the faculty as a professor at Nankai University in 2020. His research is focused on single-molecule device physics and dynamics.



Xuefeng Guo received his B.S. degree in 1998 from Beijing Normal University and his Ph.D. degree in 2004 from Institute of Chemistry, Chinese Academy of Sciences, Beijing. From 2004 to 2007, he was a postdoc at the Columbia University Nanocenter. He joined the

faculty as a professor under "Peking 100-Talent" Program at Peking University in 2008. His current research is focused on functional nanometer/molecular devices.

ACKNOWLEDGMENTS

We acknowledge primary financial supports from the National Key R&D Program of China (Nos. 2017YFA0204901, 2021YFA1200101, and 2021YFA1200102), the National Natural Science Foundation of China (Nos. 22150013, 22173050, 21727806, and 21933001), the Tencent Foundation through the XPLOER PRIZE, "Frontiers Science Center for New Organic Matter" at Nankai University (No. 63181206), the Natural Science Foundation of Beijing (No. 2222009), and Beijing National Laboratory for Molecular Sciences (No. BNLMS202105).

REFERENCES

- (1) Xin, N.; Guan, J.; Zhou, C.; Chen, X.; Gu, C.; Li, Y.; Ratner, M. A.; Nitzan, A.; Stoddart, J. F.; Guo, X. Concepts in the Design and Engineering of Single-Molecule Electronic Devices. *Nat. Rev. Phys.* **2019**, *1*, 211–230.
- (2) Gehring, P.; Thijssen, J. M.; van der Zant, H. S. J. Single-Molecule Quantum-Transport Phenomena in Break Junctions. *Nat. Rev. Phys.* **2019**, *1*, 381–396.
- (3) Chen, H.; Fraser Stoddart, J. From Molecular to Supramolecular Electronics. *Nat. Rev. Mater.* **2021**, *6*, 804–828.
- (4) Qiu, K.; Fato, T. P.; Yuan, B.; Long, Y. T. Toward Precision Measurement and Manipulation of Single-Molecule Reactions by a Confined Space. *Small* **2019**, *15*, e1805426.
- (5) Perrin, M. L.; Burzuri, E.; van der Zant, H. S. Single-Molecule Transistors. *Chem. Soc. Rev.* **2015**, *44*, 902–919.
- (6) Sun, L.; Diaz-Fernandez, Y. A.; Gschneidner, T. A.; Westerlund, F.; Lara-Avila, S.; Moth-Poulsen, K. Single-Molecule Electronics: From Chemical Design to Functional Devices. *Chem. Soc. Rev.* **2014**, *43*, 7378–7411.
- (7) Zhuang, X.; Bartley, L. E.; Babcock, H. P.; Russell, R.; Ha, T.; Herschlag, D.; Chu, S. A Single-Molecule Study of RNA Catalysis and Folding. *Science* **2000**, *288*, 2048–2051.
- (8) Wang, J.; Wang, Q.; Zhang, M. Development and Prospect of Near-Field Optical Measurements and Characterizations. *Front. Optoelectron.* **2012**, *5*, 171–181.
- (9) Halpern, A. R.; Wood, J. B.; Wang, Y.; Corn, R. M. Single-Nanoparticle near-Infrared Surface Plasmon Resonance Microscopy for Real-Time Measurements of DNA Hybridization Adsorption. *ACS Nano* **2014**, *8*, 1022–1230.
- (10) Imada, H.; Imai-Imada, M.; Miwa, K.; Yamane, H.; Iwasa, T.; Tanaka, Y.; Toriumi, N.; Kimura, K.; Yokoshi, N.; Muranaka, A.; Uchiyama, M.; Taketsugu, T.; Kato, Y. K.; Ishihara, H.; Kim, Y. Single-Molecule Laser Nanospectroscopy with Micro-Electron Volt Energy Resolution. *Science* **2021**, *373*, 95–98.
- (11) Neuman, K. C.; Nagy, A. Single-Molecule Force Spectroscopy: Optical Tweezers, Magnetic Tweezers and Atomic Force Microscopy. *Nat. Methods* **2008**, *5*, 491–505.
- (12) Fu, B.; Mosquera, M. A.; Schatz, G. C.; Ratner, M. A.; Hsu, L. Y. Photoinduced Anomalous Coulomb Blockade and the Role of Triplet States in Electron Transport through an Irradiated Molecular Transistor. *Nano Lett.* **2018**, *18*, 5015–5023.
- (13) Parks, J. J.; Champagne, A. R.; Costi, T. A.; Shum, W. W.; Pasupathy, A. N.; Neuscamman, E.; Flores-Torres, S.; Cornaglia, P. S.; Aligia, A. A.; Balseiro, C. A.; Chan, G. K.; Abruna, H. D.; Ralph, D. C. Mechanical Control of Spin States in Spin-1 Molecules and the Underscreened Kondo Effect. *Science* **2010**, *328*, 1370–1373.
- (14) Aravena, D.; Ruiz, E. Coherent Transport through Spin-Crossover Single Molecules. *J. Am. Chem. Soc.* **2012**, *134*, 777–779.
- (15) Kuang, G.; Zhang, Q.; Lin, T.; Pang, R.; Shi, X.; Xu, H.; Lin, N. Mechanically-Controlled Reversible Spin Crossover of Single Ferroporphyrin Molecules. *ACS Nano* **2017**, *11*, 6295–6300.

- (16) Meng, L.; Xin, N.; Wang, J.; Xu, J.; Ren, S.; Yan, Z.; Zhang, M.; Shen, C.; Zhang, G.; Guo, X.; Meng, S. Atomically Precise Engineering of Single-Molecule Stereoelectronic Effect. *Angew. Chem., Int. Ed.* **2021**, *60*, 12274–12278.
- (17) Xin, N.; Wang, J.; Jia, C.; Liu, Z.; Zhang, X.; Yu, C.; Li, M.; Wang, S.; Gong, Y.; Sun, H.; Zhang, G.; Liu, Z.; Zhang, G.; Liao, J.; Zhang, D.; Guo, X. Stereoelectronic Effect-Induced Conductance Switching in Aromatic Chain Single-Molecule Junctions. *Nano Lett.* **2017**, *17*, 856–861.
- (18) Aviram, A.; Ratner, M. A. Molecular Rectifiers. *Chem. Phys. Lett.* **1974**, *29*, 277–283.
- (19) Meng, F.; Hervault, Y. M.; Shao, Q.; Hu, B.; Norel, L.; Rigaut, S.; Chen, X. Orthogonally Modulated Molecular Transport Junctions for Resettable Electronic Logic Gates. *Nat. Commun.* **2014**, *5*, 3023.
- (20) Li, H. B.; Tebikachew, B. E.; Wiberg, C.; Moth-Poulsen, K.; Hihath, J. A Memristive Element Based on an Electrically Controlled Single-Molecule Reaction. *Angew. Chem., Int. Ed.* **2020**, *59*, 11641–11646.
- (21) Jia, C.; Migliore, A.; Xin, N.; Huang, S.; Wang, J.; Yang, Q.; Wang, S.; Chen, H.; Wang, D.; Feng, B.; Liu, Z.; Zhang, G.; Qu, D. H.; Tian, H.; Ratner, M. A.; Xu, H. Q.; Nitzan, A.; Guo, X. Covalently Bonded Single-Molecule Junctions with Stable and Reversibly Photoswitched Conductivity. *Science* **2016**, *352*, 1443–1445.
- (22) Zhang, G. P.; Xie, Z.; Song, Y.; Hu, G. C.; Wang, C. K. Molecular-Length Induced Inversion of Rectification in Diblock Pyrimidinyl-Phenyl Molecular Junctions. *Chem. Phys. Lett.* **2014**, *591*, 296–300.
- (23) Zhang, Z.; Zhang, J.; Kwong, G.; Li, J.; Fan, Z.; Deng, X.; Tang, G. All-Carbon Sp²-Sp³ Hybrid Structures: Geometrical Properties, Current Rectification, and Current Amplification. *Sci. Rep.* **2013**, *3*, 2575.
- (24) Richter, S.; Mentovich, E.; Elnathan, R. Realization of Molecular-Based Transistors. *Adv. Mater.* **2018**, *30*, e1706941.
- (25) Hwang, J.; Pototschnig, M.; Lettow, R.; Zumofen, G.; Renn, A.; Gotzinger, S.; Sandoghdar, V. A Single-Molecule Optical Transistor. *Nature* **2009**, *460*, 76–80.
- (26) Roch, N.; Florens, S.; Bouchiat, V.; Wernsdorfer, W.; Balestro, F. Quantum Phase Transition in a Single-Molecule Quantum Dot. *Nature* **2008**, *453*, 633–637.
- (27) Xiang, D.; Wang, X.; Jia, C.; Lee, T.; Guo, X. Molecular-Scale Electronics: From Concept to Function. *Chem. Rev.* **2016**, *116*, 4318–4440.
- (28) Zwick, P.; Dulic, D.; van der Zant, H. S. J.; Mayor, M. Porphyrins as Building Blocks for Single-Molecule Devices. *Nanoscale* **2021**, *13*, 15500–15525.
- (29) Kroto, H. W.; Heath, J. R.; O'Brien, S. C.; Curl, R. F.; Smalley, R. E. C₆₀: Buckminsterfullerene. *Nature* **1985**, *318*, 162–163.
- (30) Krätschmer, W.; Lamb, L. D.; Fostiropoulos, K.; Huffman, D. R. Solid C₆₀: A New Form of Carbon. *Nature* **1990**, *347*, 354–358.
- (31) Wienk, M. M.; Kroon, J. M.; Verhees, W. J. H.; Knol, J.; Hummelen, J. C.; Van Hal, P. A.; Janssen, R. A. J. Efficient Methano[70]Fullerene/MDMO-PPV Bulk Heterojunction Photovoltaic Cells. *Angew. Chem., Int. Ed.* **2003**, *42*, 3371–3375.
- (32) Thompson, B. C.; Fréchet, J. M. J. Polymer–Fullerene Composite Solar Cells. *Angew. Chem., Int. Ed.* **2008**, *47*, 58–77.
- (33) He, Y.; Chen, H.-Y.; Hou, J.; Li, Y. Indene-C₆₀ Bisadduct: A New Acceptor for High-Performance Polymer Solar Cells. *J. Am. Chem. Soc.* **2010**, *132*, 1377–1382.
- (34) He, Y.; Zhao, G.; Peng, B.; Li, Y. High-Yield Synthesis and Electrochemical and Photovoltaic Properties of Indene-C₇₀ Bisadduct. *Adv. Funct. Mater.* **2010**, *20*, 3383–3389.
- (35) Zhao, G.; He, Y.; Li, Y. 6.5% Efficiency of Polymer Solar Cells Based on Poly(3-Hexylthiophene) and Indene-C₆₀ Bisadduct by Device Optimization. *Adv. Mater.* **2010**, *22*, 4355–4358.
- (36) Kanbara, T.; Shibata, K.; Fujiki, S.; Kubozono, Y.; Kashino, S.; Urisu, T.; Sakai, M.; Fujiwara, A.; Kumashiro, R.; Tanigaki, K. N-Channel Field Effect Transistors with Fullerene Thin Films and Their Application to a Logic Gate Circuit. *Chem. Phys. Lett.* **2003**, *379*, 223–229.
- (37) Kobayashi, S.-I.; Mori, S.; Iida, S.; Ando, H.; Takenobu, T.; Taguchi, Y.; Fujiwara, A.; Taninaka, A.; Shinohara, H.; Iwasa, Y. Conductivity and Field Effect Transistor of La₂@C₈₀ Metallofullerene. *J. Am. Chem. Soc.* **2003**, *125*, 8116–8117.
- (38) Nagano, T.; Kuwahara, E.; Takayanagi, T.; Kubozono, Y.; Fujiwara, A. Fabrication and Characterization of Field-Effect Transistor Device with C_{2v} Isomer of Pr@C₈₂. *Chem. Phys. Lett.* **2005**, *409*, 187–191.
- (39) Tan, J.; Sorensen, J.; Dong, H.; Hu, W. Fullerene-Derivative as Interlayer for High Performance Organic Thin-Film Transistors. *J. Mater. Chem. C* **2018**, *6*, 6052–6057.
- (40) Zhao, X.; Liu, T.; Shi, W.; Hou, X.; Liu, Z.; Dennis, T. J. S. Understanding Charge Transport in Endohedral Fullerene Single-Crystal Field-Effect Transistors. *J. Phys. Chem. C* **2018**, *122*, 8822–8828.
- (41) Sato, S.; Nikawa, H.; Seki, S.; Wang, L.; Luo, G.; Lu, J.; Haranaka, M.; Tsuchiya, T.; Nagase, S.; Akasaka, T. A Co-Crystal Composed of the Paramagnetic Endohedral Metallofullerene La@C₈₂ and a Nickel Porphyrin with High Electron Mobility. *Angew. Chem., Int. Ed.* **2012**, *51*, 1589–1591.
- (42) Yue, D.; Cui, R.; Ruan, X.; Huang, H.; Guo, X.; Wang, Z.; Gao, X.; Yang, S.; Dong, J.; Yi, F.; Sun, B. A Novel Organic Electrical Memory Device Based on the Metallofullerene-Grafted Polymer (Gd@C₈₂-PVK). *Org. Electron.* **2014**, *15*, 3482–3486.
- (43) Lee, S. K.; Buerkle, M.; Yamada, R.; Asai, Y.; Tada, H. Thermoelectricity at the Molecular Scale: A Large Seebeck Effect in Endohedral Metallofullerenes. *Nanoscale* **2015**, *7*, 20497–20502.
- (44) Rincon-Garcia, L.; Ismael, A. K.; Evangeli, C.; Grace, I.; Rubio-Bollinger, G.; Porfyrakis, K.; Agrait, N.; Lambert, C. J. Molecular Design and Control of Fullerene-Based Bi-Thermoelectric Materials. *Nat. Mater.* **2016**, *15*, 289–293.
- (45) Mallik, S.; Mattauch, S.; Dalai, M. K.; Bruckel, T.; Bedanta, S. Effect of Magnetic Fullerene on Magnetization Reversal Created at the Fe/C₆₀ Interface. *Sci. Rep.* **2018**, *8*, 5515.
- (46) Joachim, C.; Gimzewski, J. K.; Schlittler, R. R.; Chavy, C. Electronic Transparency of a Single C₆₀ Molecule. *Phys. Rev. Lett.* **1995**, *74*, 2102–2105.
- (47) Park, H.; Park, J.; Lim, A. K.; Anderson, E. H.; Alivisatos, A. P.; McEuen, P. L. Nanomechanical Oscillations in a Single-C₆₀ Transistor. *Nature* **2000**, *407*, 57–60.
- (48) Champagne, A. R.; Pasupathy, A. N.; Ralph, D. C. Mechanically Adjustable and Electrically Gated Single-Molecule Transistors. *Nano Lett.* **2005**, *5*, 305–308.
- (49) Popov, A. A.; Yang, S.; Dunsch, L. Endohedral Fullerenes. *Chem. Rev.* **2013**, *113*, 5989–6113.
- (50) Yang, S.; Wei, T.; Jin, F. When Metal Clusters Meet Carbon Cages: Endohedral Clusterfullerenes. *Chem. Soc. Rev.* **2017**, *46*, 5005–5058.
- (51) Chandler, H. J.; Stefanou, M.; Campbell, E. E. B.; Schaub, R. Li@C₆₀ as a Multi-State Molecular Switch. *Nat. Commun.* **2019**, *10*, 2283.
- (52) Xu, H.; Wang, Z.; Lu, Y.; Wei, S.; Liu, X.; Wang, L. Construction of a Molecular Switch Based on Two Metastable States of Fullerene on Cu(111). *J. Phys. Chem. C* **2020**, *124*, 11158–11164.
- (53) Zhang, K.; Wang, C.; Zhang, M.; Bai, Z.; Xie, F. F.; Tan, Y. Z.; Guo, Y.; Hu, K. J.; Cao, L.; Zhang, S.; Tu, X.; Pan, D.; Kang, L.; Chen, J.; Wu, P.; Wang, X.; Wang, J.; Liu, J.; Song, Y.; Wang, G.; Song, F.; Ji, W.; Xie, S. Y.; Shi, S. F.; Reed, M. A.; Wang, B. A Gd@C₈₂ Single-Molecule Electret. *Nat. Nanotechnol.* **2020**, *15*, 1019–1024.
- (54) Kim, Y.; Jeong, W.; Kim, K.; Lee, W.; Reddy, P. Electrostatic Control of Thermoelectricity in Molecular Junctions. *Nat. Nanotechnol.* **2014**, *9*, 881–885.
- (55) Gehring, P.; Harzheim, A.; Spiece, J.; Sheng, Y.; Rogers, G.; Evangeli, C.; Mishra, A.; Robinson, B. J.; Porfyrakis, K.; Warner, J. H.; Kolosov, O. V.; Briggs, G. A. D.; Mol, J. A. Field-Effect Control of Graphene-Fullerene Thermoelectric Nanodevices. *Nano Lett.* **2017**, *17*, 7055–7061.
- (56) Randel, J. C.; Niestemski, F. C.; Botello-Mendez, A. R.; Mar, W.; Ndabashimiye, G.; Melinte, S.; Dahl, J. E.; Carlson, R. M.; Butova,

- E. D.; Fokin, A. A.; Schreiner, P. R.; Charlier, J. C.; Manoharan, H. C. Unconventional Molecule-Resolved Current Rectification in Diamondoid-Fullerene Hybrids. *Nat. Commun.* **2014**, *5*, 4877.
- (57) Tan, Z.; Zhang, D.; Tian, H. R.; Wu, Q.; Hou, S.; Pi, J.; Sadeghi, H.; Tang, Z.; Yang, Y.; Liu, J.; Tan, Y. Z.; Chen, Z. B.; Shi, J.; Xiao, Z.; Lambert, C.; Xie, S. Y.; Hong, W. Atomically Defined Angstrom-Scale All-Carbon Junctions. *Nat. Commun.* **2019**, *10*, 1748.
- (58) Reed, M. A.; Zhou, C.; Muller, C. J.; Burgin, T. P.; Tour, J. M. Conductance of a Molecular Junction. *Science* **1997**, *278*, 252–254.
- (59) Zhou, C.; Muller, C. J.; Deshpande, M. R.; Sleight, J. W.; Reed, M. A. Microfabrication of a Mechanically Controllable Break Junction in Silicon. *Appl. Phys. Lett.* **1995**, *67*, 1160–1162.
- (60) Pasupathy, A. N.; Park, J.; Chang, C.; Soldatov, A. V.; Lebedkin, S.; Bialczak, R. C.; Grose, J. E.; Donev, L. A.; Sethna, J. P.; Ralph, D. C.; McEuen, P. L. Vibration-Assisted Electron Tunneling in C_{140} Transistors. *Nano Lett.* **2005**, *5*, 203–207.
- (61) Winkelmann, C. B.; Roch, N.; Wernsdorfer, W.; Bouchiat, V.; Balestro, F. Superconductivity in a Single- C_{60} Transistor. *Nat. Phys.* **2009**, *5*, 876–879.
- (62) Park, H.; Lim, A. K. L.; Alivisatos, A. P.; Park, J.; McEuen, P. L. Fabrication of Metallic Electrodes with Nanometer Separation by Electromigration. *Appl. Phys. Lett.* **1999**, *75*, 301–303.
- (63) O'Neill, K.; Osorio, E. A.; van der Zant, H. S. J. Self-Breaking in Planar Few-Atom Au Constrictions for Nanometer-Spaced Electrodes. *Appl. Phys. Lett.* **2007**, *90*, 133109.
- (64) Houck, A. A.; Labaziewicz, J.; Chan, E. K.; Folk, J. A.; Chuang, I. L. Kondo Effect in Electromigrated Gold Break Junctions. *Nano Lett.* **2005**, *5*, 1685–1688.
- (65) Kasumov, A. Y.; Tsukagoshi, K.; Kawamura, M.; Kobayashi, T.; Aoyagi, Y.; Senba, K.; Kodama, T.; Nishikawa, H.; Ikemoto, I.; Kikuchi, K.; Volkov, V. T.; Kasumov, Y. A.; Deblock, R.; Guéron, S.; Bouchiat, H. Proximity Effect in a Superconductor-Metallofullerene-Superconductor Molecular Junction. *Phys. Rev. B* **2005**, *72*, 033414.
- (66) Yoshida, K.; Hamada, I.; Sakata, S.; Umeno, A.; Tsukada, M.; Hirakawa, K. Gate-Tunable Large Negative Tunnel Magnetoresistance in Ni- C_{60} -Ni Single Molecule Transistors. *Nano Lett.* **2013**, *13*, 481–485.
- (67) Lau, C. S.; Sadeghi, H.; Rogers, G.; Sangtarash, S.; Dallas, P.; Porfyrakis, K.; Warner, J.; Lambert, C. J.; Briggs, G. A.; Mol, J. A. Redox-Dependent Franck-Condon Blockade and Avalanche Transport in a Graphene-Fullerene Single-Molecule Transistor. *Nano Lett.* **2016**, *16*, 170–176.
- (68) Prins, F.; Barreiro, A.; Ruitenbergh, J. W.; Seldenthuis, J. S.; Aliaga-Alcalde, N.; Vandersypen, L. M.; van der Zant, H. S. Room-Temperature Gating of Molecular Junctions Using Few-Layer Graphene Nanogap Electrodes. *Nano Lett.* **2011**, *11*, 4607–4611.
- (69) Guo, X.; Small, J. P.; Klare, J. E.; Wang, Y.; Purewal, M. S.; Tam, I. W.; Hong, B. H.; Caldwell, R.; Huang, L.; O'Brien, S.; Yan, J.; Breslow, R.; Wind, S. J.; Hone, J.; Kim, P.; Nuckolls, C. Covalently Bridging Gaps in Single-Walled Carbon Nanotubes with Conducting Molecules. *Science* **2006**, *311*, 356–359.
- (70) Cao, Y.; Dong, S.; Liu, S.; He, L.; Gan, L.; Yu, X.; Steigerwald, M. L.; Wu, X.; Liu, Z.; Guo, X. Building High-Throughput Molecular Junctions Using Indented Graphene Point Contacts. *Angew. Chem., Int. Ed.* **2012**, *51*, 12228–12232.
- (71) Lau, C. S.; Mol, J. A.; Warner, J. H.; Briggs, G. A. Nanoscale Control of Graphene Electrodes. *Phys. Chem. Chem. Phys.* **2014**, *16*, 20398–20401.
- (72) Candini, A.; Richter, N.; Convertino, D.; Coletti, C.; Balestro, F.; Wernsdorfer, W.; Klau, M.; Affronte, M. Electroburning of Few-Layer Graphene Flakes, Epitaxial Graphene, and Turbostratic Graphene Discs in Air and under Vacuum. *Beilstein J. Nanotechnol.* **2015**, *6*, 711–719.
- (73) El Abbassi, M.; Posa, L.; Makk, P.; Nef, C.; Thodkar, K.; Halbritter, A.; Calame, M. From Electroburning to Sublimation: Substrate and Environmental Effects in the Electrical Breakdown Process of Monolayer Graphene. *Nanoscale* **2017**, *9*, 17312–17317.
- (74) Xin, N.; Jia, C.; Wang, J.; Wang, S.; Li, M.; Gong, Y.; Zhang, G.; Zhu, D.; Guo, X. Thermally Activated Tunneling Transition in a Photoswitchable Single-Molecule Electrical Junction. *J. Phys. Chem. Lett.* **2017**, *8*, 2849–2854.
- (75) Xin, N.; Li, X.; Jia, C.; Gong, Y.; Li, M.; Wang, S.; Zhang, G.; Yang, J.; Guo, X. Tuning Charge Transport in Aromatic-Ring Single-Molecule Junctions via Ionic-Liquid Gating. *Angew. Chem., Int. Ed.* **2018**, *57*, 14026–14031.
- (76) Meng, L.; Xin, N.; Hu, C.; Wang, J.; Gui, B.; Shi, J.; Wang, C.; Shen, C.; Zhang, G.; Guo, H.; Meng, S.; Guo, X. Side-Group Chemical Gating via Reversible Optical and Electric Control in a Single Molecule Transistor. *Nat. Commun.* **2019**, *10*, 1450.
- (77) Gu, C.; Hu, C.; Wei, Y.; Lin, D.; Jia, C.; Li, M.; Su, D.; Guan, J.; Xia, A.; Xie, L.; Nitzan, A.; Guo, H.; Guo, X. Label-Free Dynamic Detection of Single-Molecule Nucleophilic-Substitution Reactions. *Nano Lett.* **2018**, *18*, 4156–4162.
- (78) Guan, J.; Jia, C.; Li, Y.; Liu, Z.; Wang, J.; Yang, Z.; Gu, C.; Su, D.; Houk, K. N.; Zhang, D.; Guo, X. Direct Single-Molecule Dynamic Detection of Chemical Reactions. *Sci. Adv.* **2018**, *4*, eaar2177.
- (79) Yang, C.; Liu, Z.; Li, Y.; Zhou, S.; Lu, C.; Guo, Y.; Ramirez, M.; Zhang, Q.; Li, Y.; Liu, Z.; Houk, K. N.; Zhang, D.; Guo, X. Electric Field-Catalyzed Single-Molecule Diels-Alder Reaction Dynamics. *Sci. Adv.* **2021**, *7*, eabf0689.
- (80) Yang, C.; Zhang, L.; Li, H.; Guo, Y.; Jia, C.; Zhu, W.; Mo, F.; Guo, X. Single-Molecule Electrical Spectroscopy of Organocatalysis. *Matter* **2021**, *4*, 2874–2885.
- (81) Nirmalraj, P.; La Rosa, A.; Thompson, D.; Sousa, M.; Martin, N.; Gotsmann, B.; Riel, H. Fingerprinting Electronic Molecular Complexes in Liquid. *Sci. Rep.* **2016**, *6*, 19009.
- (82) Martin, C. A.; Ding, D.; Sorensen, J. K.; Bjornholm, T.; van Ruitenbeek, J. M.; van der Zant, H. S. Fullerene-Based Anchoring Groups for Molecular Electronics. *J. Am. Chem. Soc.* **2008**, *130*, 13198–13199.
- (83) Parks, J. J.; Champagne, A. R.; Hutchison, G. R.; Flores-Torres, S.; Abruna, H. D.; Ralph, D. C. Tuning the Kondo Effect with a Mechanically Controllable Break Junction. *Phys. Rev. Lett.* **2007**, *99*, 026601.
- (84) Johansson, M. K.; Maxwell, A. J.; Gray, S. M.; Bruhwiler, P. A.; Mancini, D. C.; Johansson, L. S.; Martensson, N. Scanning Tunneling Microscopy of $C_{60}/Al(111)-6 \times 6$: Inequivalent Molecular Sites and Electronic Structures. *Phys. Rev. B: Condens. Matter* **1996**, *54*, 13472–13475.
- (85) Porath, D.; Levi, Y.; Tarabiah, M.; Millo, O. Tunneling Spectroscopy of Isolated C_{60} Molecules in the Presence of Charging Effects. *Phys. Rev. B* **1997**, *56*, 9829–9833.
- (86) Dunn, A. W.; Svensson, E. D.; Dekker, C. Scanning Tunneling Spectroscopy of C_{60} Adsorbed on $Si(100)-(2 \times 1)$. *Surf. Sci.* **2002**, *498*, 237–243.
- (87) Lu, X.; Grobis, M.; Khoo, K. H.; Louie, S. G.; Crommie, M. F. Charge Transfer and Screening in Individual C_{60} Molecules on Metal Substrates: A Scanning Tunneling Spectroscopy and Theoretical Study. *Phys. Rev. B* **2004**, *70*, 115418.
- (88) Tang, Q.; Zhang, G.; Jiang, B.; Ji, D.; Kong, H.; Riehemann, K.; Ji, Q.; Fuchs, H. Self-Assembled Fullerene (C_{60})-Pentacene Superstructures for Photodetectors. *SmartMat* **2021**, *2*, 109–118.
- (89) Boyd, P. D.; Reed, C. A. Fullerene-Porphyrin Constructs. *Acc. Chem. Res.* **2005**, *38*, 235–242.
- (90) Zhang, J.; Tan, J.; Ma, Z.; Xu, W.; Zhao, G.; Geng, H.; Di, C.; Hu, W.; Shuai, Z.; Singh, K.; Zhu, D. Fullerene/Sulfur-Bridged Annulene Cocrystals: Two-Dimensional Segregated Heterojunctions with Ambipolar Transport Properties and Photoresponsivity. *J. Am. Chem. Soc.* **2013**, *135*, 558–561.
- (91) Zheng, S.; Zhong, J.; Matsuda, W.; Jin, P.; Chen, M.; Akasaka, T.; Tsukagoshi, K.; Seki, S.; Zhou, J.; Lu, X. Fullerene/Cobalt Porphyrin Charge-Transfer Cocrystals: Excellent Thermal Stability and High Mobility. *Nano Res.* **2018**, *11*, 1917–1927.
- (92) Khadem Hosseini, V.; Ahmadi, M. T.; Ismail, R. Analysis and Modeling of Fullerene Single Electron Transistor Based on Quantum Dot Arrays at Room Temperature. *J. Electron. Mater.* **2018**, *47*, 4799–4806.

- (93) Sergeev, D. Single Electron Transistor Based on Endohedral Metallofullerenes Me@C₆₀ (Me = Li, Na, K). *J. Nano-Electron. Phys.* **2020**, *12*, 03017-1.
- (94) Okamura, N.; Yoshida, K.; Sakata, S.; Hirakawa, K. Electron Transport in Endohedral Metallofullerene Ce@C₈₂ Single-Molecule Transistors. *Appl. Phys. Lett.* **2015**, *106*, 043108.
- (95) Du, S.; Yoshida, K.; Zhang, Y.; Hamada, I.; Hirakawa, K. Terahertz Dynamics of Electron-Vibron Coupling in Single Molecules with Tunable Electrostatic Potential. *Nat. Photonics* **2018**, *12*, 608–612.
- (96) Pasupathy, A. N.; Bialczak, R. C.; Martinek, J.; Grose, J. E.; Donev, L. A.; McEuen, P. L.; Ralph, D. C. The Kondo Effect in the Presence of Ferromagnetism. *Science* **2004**, *306*, 86–89.
- (97) Cornia, A.; Seneor, P. Spintronics: The Molecular Way. *Nat. Mater.* **2017**, *16*, 505–506.
- (98) Kondo, J. Resistance Minimum in Dilute Magnetic Alloys. *Prog. Theor. Phys.* **1964**, *32*, 37–49.
- (99) Frisenda, R.; Gaudenzi, R.; Franco, C.; Mas-Torrent, M.; Rovira, C.; Veciana, J.; Alcon, I.; Bromley, S. T.; Burzuri, E.; van der Zant, H. S. Kondo Effect in a Neutral and Stable All Organic Radical Single Molecule Break Junction. *Nano Lett.* **2015**, *15*, 3109–3114.
- (100) Appelt, W. H.; Droghetti, A.; Chioncel, L.; Radonjic, M. M.; Munoz, E.; Kirchner, S.; Vollhardt, D.; Rungger, I. Predicting the Conductance of Strongly Correlated Molecules: The Kondo Effect in Perchlorotriphenylmethyl/Au Junctions. *Nanoscale* **2018**, *10*, 17738–17750.
- (101) Mahan, G. D.; Sofo, J. O. The Best Thermoelectric. *Proc. Natl. Acad. Sci. U.S.A.* **1996**, *93*, 7436–7439.
- (102) Finch, C. M.; García-Suárez, V. M.; Lambert, C. J. Giant Thermopower and Figure of Merit in Single-Molecule Devices. *Phys. Rev. B* **2009**, *79*, 033405.
- (103) Bergfield, J. P.; Solis, M. A.; Stafford, C. A. Giant Thermoelectric Effect from Transmission Supernodes. *ACS Nano* **2010**, *4*, 5314–20.
- (104) Karlström, O.; Linke, H.; Karlström, G.; Wacker, A. Increasing Thermoelectric Performance Using Coherent Transport. *Phys. Rev. B* **2011**, *84*, 113415.
- (105) Yee, S. K.; Malen, J. A.; Majumdar, A.; Segalman, R. A. Thermoelectricity in Fullerene-Metal Heterojunctions. *Nano Lett.* **2011**, *11*, 4089–4094.
- (106) Zhao, Y.; Liu, L.; Zhang, F.; Di, C. a.; Zhu, D. Advances in Organic Thermoelectric Materials and Devices for Smart Applications. *SmartMat* **2021**, *2*, 426–445.
- (107) Kobayashi, K.; Nagase, S.; Akasaka, T. Endohedral Dimetallofullerenes Sc₂@C₈₄ and La₂@C₈₀. Are the Metal Atoms Still inside the Fullerene Cages? *Chem. Phys. Lett.* **1996**, *261*, 502–506.
- (108) Akasaka, T.; Nagase, S.; Kobayashi, K.; Wälchli, M.; Yamamoto, K.; Funasaka, H.; Kako, M.; Hoshino, T.; Erata, T. 13c And139la Nmr Studies of La₂@C₈₀: First Evidence for Circular Motion of Metal Atoms in Endohedral Dimetallofullerenes. *Angew. Chem., Int. Ed.* **1997**, *36*, 1643–1645.
- (109) Shimotani, H.; Ito, T.; Iwasa, Y.; Taninaka, A.; Shinohara, H.; Nishibori, E.; Takata, M.; Sakata, M. Quantum Chemical Study on the Configurations of Encapsulated Metal Ions and the Molecular Vibration Modes in Endohedral Dimetallofullerene La₂@C₈₀. *J. Am. Chem. Soc.* **2004**, *126*, 364–369.
- (110) Yamada, M.; Nakahodo, T.; Wakahara, T.; Tsuchiya, T.; Maeda, Y.; Akasaka, T.; Kako, M.; Yoza, K.; Horn, E.; Mizorogi, N.; Kobayashi, K.; Nagase, S. Positional Control of Encapsulated Atoms inside a Fullerene Cage by Exohedral Addition. *J. Am. Chem. Soc.* **2005**, *127*, 14570–14571.
- (111) Yamada, M.; Wakahara, T.; Nakahodo, T.; Tsuchiya, T.; Maeda, Y.; Akasaka, T.; Yoza, K.; Horn, E.; Mizorogi, N.; Nagase, S. Synthesis and Structural Characterization of Endohedral Pyrrolidino-dimetallofullerene: La₂@C₈₀(CH₂)₂NTrt. *J. Am. Chem. Soc.* **2006**, *128*, 1402–1403.
- (112) Pérez-Jiménez, Á. J. Molecular Electronics with Endohedral Metallofullerenes: The Test Case of La₂@C₈₀ Nanojunctions. *J. Phys. Chem. C* **2007**, *111*, 17640–17645.
- (113) Jorn, R.; Zhao, J.; Petek, H.; Seideman, T. Current-Driven Dynamics in Molecular Junctions: Endohedral Fullerenes. *ACS Nano* **2011**, *5*, 7858–7865.
- (114) Yasutake, Y.; Shi, Z.; Okazaki, T.; Shinohara, H.; Majima, Y. Single Molecular Orientation Switching of an Endohedral Metallofullerene. *Nano Lett.* **2005**, *5*, 1057–1060.
- (115) Huang, T.; Zhao, J.; Feng, M.; Popov, A. A.; Yang, S.; Dunsch, L.; Petek, H. A Molecular Switch Based on Current-Driven Rotation of an Encapsulated Cluster within a Fullerene Cage. *Nano Lett.* **2011**, *11*, 5327–5332.
- (116) Li, T.; Hauptmann, J. R.; Wei, Z.; Petersen, S.; Bovet, N.; Vosch, T.; Nygård, J.; Hu, W.; Bjørnholm, T.; Nørgaard, K.; Laursen, B. W. Solution-Processed Ultrathin Chemically Derived Graphene Films as Soft Top Contacts for Solid-State Molecular Electronic Junctions. *Adv. Mater.* **2012**, *24*, 1333–1339.
- (117) Wang, Z.; Dong, H.; Li, T.; Hviid, R.; Zou, Y.; Wei, Z.; Fu, X.; Wang, E.; Zhen, Y.; Nørgaard, K.; Laursen, B. W.; Hu, W. Role of Redox Centre in Charge Transport Investigated by Novel Self-Assembled Conjugated Polymer Molecular Junctions. *Nat. Commun.* **2015**, *6*, 7478.
- (118) Dong, H.; Hu, W. Multilevel Investigation of Charge Transport in Conjugated Polymers. *Acc. Chem. Res.* **2016**, *49*, 2435–2443.
- (119) Otsubo, T.; Aso, Y.; Takimiya, K. Functional Oligothiophenes as Advanced Molecular Electronic Materials. *J. Mater. Chem.* **2002**, *12*, 2565–2575.
- (120) Matsuo, Y.; Ichiki, T.; Nakamura, E. Molecular Photoelectric Switch Using a Mixed SAM of Organic [60]Fullerene and [70]Fullerene Doped with a Single Iron Atom. *J. Am. Chem. Soc.* **2011**, *133*, 9932–9937.
- (121) Abrusci, A.; Stranks, S. D.; Docampo, P.; Yip, H.-L.; Jen, A. K.-Y.; Snaith, H. J. High-Performance Perovskite-Polymer Hybrid Solar Cells via Electronic Coupling with Fullerene Monolayers. *Nano Lett.* **2013**, *13*, 3124–3128.
- (122) Stefan-Van Staden, R.-I. Enantioselective Surface Plasmon Resonance Sensor Based on C₆₀fullerene-Glutathione Self-Assembled Monolayer (SAM). *Chirality* **2014**, *26*, 129–131.
- (123) Uji, H.; Tanaka, K.; Kimura, S. O₂-Triggered Directional Switching of Photocurrent in Self-Assembled Monolayer Composed of Porphyrin- and Fullerene-Terminated Helical Peptides on Gold. *J. Phys. Chem. C* **2016**, *120*, 3684–3689.
- (124) Valles-Pelarda, M.; Hames, B. C.; García-Benito, I.; Almora, O.; Molina-Ontoria, A.; Sánchez, R. S.; Garcia-Belmonte, G.; Martín, N.; Mora-Sero, I. Analysis of the Hysteresis Behavior of Perovskite Solar Cells with Interfacial Fullerene Self-Assembled Monolayers. *J. Phys. Chem. Lett.* **2016**, *7*, 4622–4628.
- (125) Nirmalraj, P.; Daly, R.; Martin, N.; Thompson, D. Motion of Fullerenes around Topological Defects on Metals: Implications for the Progress of Molecular Scale Devices. *ACS Appl. Mater. Interfaces* **2017**, *9*, 7897–7902.
- (126) Chen, C.-H.; Krylov, D. S.; Avdoshenko, S. M.; Liu, F.; Spree, L.; Westerström, R.; Bulbucan, C.; Studniarek, M.; Dreiser, J.; Wolter, A. U. B.; Büchner, B.; Popov, A. A. Magnetic Hysteresis in Self-Assembled Monolayers of Dy-Fullerene Single Molecule Magnets on Gold. *Nanoscale* **2018**, *10*, 11287–11292.
- (127) Booker, E. P.; Bayliss, S. L.; Jen, A.; Rao, A.; Greenham, N. C. Magnetic Field Modulation of Recombination Processes in Organic Photovoltaics. *IEEE J. Photovolt.* **2019**, *9*, 460–463.
- (128) Chen, C. H.; Spree, L.; Koutsouflakis, E.; Krylov, D. S.; Liu, F.; Brandenburg, A.; Schimmel, S.; Avdoshenko, S. M.; Fedorov, A.; Weschke, E.; Choueikani, F.; Ohresser, P.; Dreiser, J.; Büchner, B.; Popov, A. A. Magnetic Hysteresis at 10 K in Single Molecule Magnet Self-Assembled on Gold. *Adv. Sci.* **2021**, *8*, 2000777.
- (129) Krylov, D. S.; Schimmel, S.; Dubrovin, V.; Liu, F.; Nguyen, T. T. N.; Spree, L.; Chen, C. H.; Velkos, G.; Bulbucan, C.; Westerström,

- R.; Studniarek, M.; Dreiser, J.; Hess, C.; Büchner, B.; Avdoshenko, S. M.; Popov, A. A. Substrate-Independent Magnetic Bistability in Monolayers of the Single-Molecule Magnet $\text{Dy}_2\text{SCN}@C_{80}$ on Metals and Insulators. *Angew. Chem., Int. Ed.* **2020**, *59*, 5756–5764.
- (130) Paschke, F.; Birk, T.; Enenkel, V.; Liu, F.; Romankov, V.; Dreiser, J.; Popov, A. A.; Fonin, M. Exceptionally High Blocking Temperature of 17 K in a Surface-Supported Molecular Magnet. *Adv. Mater.* **2021**, *33*, 2102844.
- (131) Spree, L.; Liu, F.; Neu, V.; Rosenkranz, M.; Velkos, G.; Wang, Y.; Schiemenz, S.; Dreiser, J.; Gargiani, P.; Valvidares, M.; Chen, C. H.; Büchner, B.; Avdoshenko, S. M.; Popov, A. A. Robust Single Molecule Magnet Monolayers on Graphene and Graphite with Magnetic Hysteresis up to 28 K. *Adv. Funct. Mater.* **2021**, *31*, 2105516.
- (132) Wang, Y.; Velkos, G.; Israel, N. J.; Rosenkranz, M.; Büchner, B.; Liu, F.; Popov, A. A. Electrophilic Trifluoromethylation of Dimetallofullerene Anions En Route to Air-Stable Single-Molecule Magnets with High Blocking Temperature of Magnetization. *J. Am. Chem. Soc.* **2021**, *143*, 18139–18149.
- (133) Wakahara, T.; Kato, T.; Miyazawa, K.; Harneit, W. $\text{N}@C_{60}$ as a Structural Probe for Fullerene Nanomaterials. *Carbon* **2012**, *50*, 1709–1712.
- (134) Zhou, S.; Rasovic, I.; Briggs, G. A.; Porfyrakis, K. Synthesis of the First Completely Spin-Compatible $\text{N}@C_{60}$ Cyclopropane Derivatives by Carefully Tuning the Dbu Base Catalyst. *ChemComm* **2015**, *51*, 7096–7099.
- (135) Zhou, S.; Yuan, J.; Wang, Z. Y.; Ling, K.; Fu, P. X.; Fang, Y. H.; Wang, Y. X.; Liu, Z.; Porfyrakis, K.; Briggs, G. A. D.; Gao, S.; Jiang, S. D. Implementation of Quantum Level Addressability and Geometric Phase Manipulation in Aligned Endohedral Fullerene Qudits. *Angew. Chem., Int. Ed.* **2021**, *61* (8), e202115263.
- (136) Hu, Z.; Dong, B. W.; Liu, Z.; Liu, J. J.; Su, J.; Yu, C.; Xiong, J.; Shi, D. E.; Wang, Y.; Wang, B. W.; Ardavan, A.; Shi, Z.; Jiang, S. D.; Gao, S. Endohedral Metallofullerene as Molecular High Spin Qubit: Diverse Rabi Cycles in $\text{Gd}_2@C_{79}\text{N}$. *J. Am. Chem. Soc.* **2018**, *140*, 1123–1130.
- (137) Wang, Y.; Xiong, J.; Su, J.; Hu, Z.; Ma, F.; Sun, R.; Tan, X.; Sun, H. L.; Wang, B. W.; Shi, Z.; Gao, S. $\text{Dy}_2@C_{79}\text{N}$: A New Member of Dimetalloazafullerenes with Strong Single Molecular Magnetism. *Nanoscale* **2020**, *12*, 11130–11135.
- (138) Morton, J. J.; Tyryshkin, A. M.; Ardavan, A.; Porfyrakis, K.; Lyon, S. A.; Briggs, A. D. G. Electron Spin Relaxation of $\text{N}@C_{60}$ in CS_2 . *J. Chem. Phys.* **2006**, *124*, 014508.
- (139) Brown, R. M.; Ito, Y.; Warner, J. H.; Ardavan, A.; Shinohara, H.; Briggs, G. A. D.; Morton, J. J. L. Electron Spin Coherence in Metallofullerenes: Y, Sc, and $\text{La}@C_{82}$. *Phys. Rev. B* **2010**, *82*, 033410.
- (140) Morton, J. J. L.; Tyryshkin, A. M.; Ardavan, A.; Benjamin, S. C.; Porfyrakis, K.; Lyon, S. A.; Briggs, G. A. D. Bang-Bang Control of Fullerene Qubits Using Ultrafast Phase Gates. *Nat. Phys.* **2006**, *2*, 40–43.
- (141) Wang, Y.-X.; Liu, Z.; Fang, Y.-H.; Zhou, S.; Jiang, S.-D.; Gao, S. Coherent Manipulation and Quantum Phase Interference in a Fullerene-Based Electron Triplet Molecular Qutrit. *npj Quantum Inf.* **2021**, *7*, 32.
- (142) Harding, R. T.; Zhou, S.; Zhou, J.; Lindvall, T.; Myers, W. K.; Ardavan, A.; Briggs, G. A. D.; Porfyrakis, K.; Laird, E. A. Spin Resonance Clock Transition of the Endohedral Fullerene $^{15}\text{N}@C_{60}$. *Phys. Rev. Lett.* **2017**, *119*, 140801.
- (143) Cornes, S. P.; Zhou, S.; Porfyrakis, K. Synthesis and Epr Studies of the First Water-Soluble $\text{N}@C_{60}$ Derivative. *ChemComm* **2017**, *53*, 12742–12745.
- (144) Meng, Q.; Abella, L.; Yang, W.; Yao, Y.-R.; Liu, X.; Zhuang, J.; Li, X.; Echegoyen, L.; Autschbach, J.; Chen, N. $\text{UCN}@C_s(6)-C_{82}$: An Encapsulated Triangular Ucn Cluster with Ambiguous U Oxidation State [U(III) versus U(I)]. *J. Am. Chem. Soc.* **2021**, *143*, 16226–16234.
- (145) Liu, F.; Velkos, G.; Krylov, D. S.; Spree, L.; Zalibera, M.; Ray, R.; Samoylova, N. A.; Chen, C. H.; Rosenkranz, M.; Schiemenz, S.; Ziegs, F.; Nenkov, K.; Kostanyan, A.; Greber, T.; Wolter, A. U. B.; Richter, M.; Buchner, B.; Avdoshenko, S. M.; Popov, A. A. Air-Stable Redox-Active Nanomagnets with Lanthanide Spins Radical-Bridged by a Metal-Metal Bond. *Nat. Commun.* **2019**, *10*, 571.
- (146) Paschke, F.; Birk, T.; Avdoshenko, S. M.; Liu, F.; Popov, A. A.; Fonin, M. Imaging the Single-Electron Ln-Ln Bonding Orbital in a Dimetallofullerene Molecular Magnet. *Small* **2022**, *18*, 2105667.
- (147) Velkos, G.; Krylov, D. S.; Kirkpatrick, K.; Spree, L.; Dubrovin, V.; Büchner, B.; Avdoshenko, S. M.; Bezmelnitsyn, V.; Davis, S.; Faust, P.; Duchamp, J.; Dorn, H. C.; Popov, A. A. High Blocking Temperature of Magnetization and Giant Coercivity in the Azafullerene $\text{Tb}_2@C_{79}\text{N}$ with a Single-Electron Terbium-Terbium Bond. *Angew. Chem., Int. Ed.* **2019**, *58*, 5891–5896.
- (148) Hao, Y.; Wang, Y.; Dubrovin, V.; Avdoshenko, S. M.; Popov, A. A.; Liu, F. Caught in Phase Transition: Snapshot of the Metallofullerene $\text{Sc}_3\text{N}@C_{70}$ Rotation in the Crystal. *J. Am. Chem. Soc.* **2021**, *143*, 612–616.
- (149) Yao, Y.-R.; Roselló, Y.; Ma, L.; Puente Santiago, A. R.; Metta-Magaña, A.; Chen, N.; Rodríguez-Fortea, A.; Poblet, J. M.; Echegoyen, L. Crystallographic Characterization of $\text{U}@C_{2n}$ ($2n = 82–86$): Insights About Metal-Cage Interactions for Mono-Metallofullerenes. *J. Am. Chem. Soc.* **2021**, *143*, 15309–15318.